PHOTOCATALYTIC REDUCTION OF HEXAVALENT CHROMIUM IN AQUEOUS SOLUTIONS BY TiO_2/PAN NANOFIBERS

A Thesis

presented to

the Faculty of the Graduate School

at the University of Missouri-Columbia

In Partial Fulfillment

of the Requirements for the Degree

Master of Science

by

HANG ZHOU

Dr. Baolin Deng, Thesis Supervisor

July 2013

The undersigned, appointed by the dean of the Graduate School, have examined the thesis entitled

PHOTOCATALYTIC REDUCTION OF HEXAVALENT CHROMIUM IN AQUEOUS SOLUTIONS BY TiO_2/PAN NANOFIBERS

presented by Hang Zhou

a candidate for the degree master of science in chemical engineering,

and hereby certify that, in their opinion, it is worthy of acceptance.

Professor Baolin Deng

Professor Sheila Baker

Professor Tom Clevenger

Professor David Retzloff

ACKNOWLEDGEMENTS

I would like to express my gratitude to all those who helped me for my research and writing of this thesis.

My deepest gratitude goes first and foremost to my advisor Dr. Baolin Deng for his constant encouragement and valuable guidance in the academic studies. In the preparation of the thesis, Dr. Deng has spent much time reading through each draft and provided me with inspiring advice. Without his patient instruction, insightful criticism and expert guidance, the completion of this thesis would not have been possible.

I am grateful to my thesis committee members: Drs. Sheila Baker, David Retzloff and Thomas Clevenger who have generously provided their time and valuable suggestions to my thesis.

I gratefully acknowledge Mr. Ali Tekeei in Professor Galen Suppes' group in the Department of Chemical Engineering at University of Missouri for N_2 adsorption/desorption analysis. I would like to thank all the members of our research group for their support in my lab works. Thank you Yin Jun for your kind assistance in SEM, XRD and BET characterization, Guocheng Zhu for helping me doing the TOC test and so much lab works, Weiming Hu for teaching me how to synthesis the testing materials, and Ms. Jennifer Keyzer-Andre for the administrative works.

I am also grateful to all the friends who have given me generous support and helpful advice in the past 2 years. Without your company, the life as a student studying abroad would be much tedious and tough.

Finally, I wish to devote this thesis to my beloved family, who gave me life and love, and stand by me for 22 years.

TABLE OF CONTENTS

ACKNOWLEDGEMENTS ii

LIST OF ILLUSTRATIONS vi

LIST OF TABLES viii

Chapter 1 INTRODUCTION 1

Chapter 2 BACKGROUND AND LITERATURE REVIEW 5

2.1 TiO_2 and photocatalysis process 5

2.1.1 Basic mechanism of photocatalysis 5

2.1.2 TiO_2 nanofiber and its modification 6

2.2 Electrospinning technique 9

2.3 Degradation of Hexavalent Chromium 12

2.3.1 Cr(VI) in drinking water 12

2.3.2 Traditional treatment method for Cr(VI) 14

2.3.3 Photocatalytic reduction of Cr(VI) 16

Reference 21

Chapter 3 EXPERIMENTAL PROCEDURE AND METHODOLOGY 24

Overview 24

3.1 Materials and equipment 24

3.2 Preparation of TiO_2/PAN nanofiber 25

3.2.1 Electrospinning 25

3.2.2 Post preparation and annealing 26

3.3 Determination method of Cr(VI) 27

3.4 Removal of Cr(VI) on TiO_2/PAN Nanofibers 29

3.4.1 Adsorption of Cr(VI) by TiO_2/PAN Nanofibers 29

3.4.2 Photorcatalytic reduction of Cr(VI) by TiO_2/PAN Nanofibers 29
3.5 Data analysis and modeling..... 31
Reference 32
Chapter 4 EXPERIMENT RESULTS AND DISCUSSION 33
4.1 Characterization of TiO_2/PAN nanofibers 33
4.2 Adsorption of Cr(VI) on TiO_2/PAN Nanofibers 37
4.3 Photoreduction of Cr(VI) by TiO_2/PAN Nanofibers..... 38
4.3.1 Influence of pH 40
4.3.2 Influence of light source 46
4.3.3 The impact of humic acid (HA)..... 50
Reference 56
Chapter 5 CONCLUSIONS AND PERSPECTIVE 61
5.1 Conclusions 61
5.2 Recommendation and future research 62
Appendix..... 63

LIST OF ILLUSTRATIONS

Figure Page

Figure 2.1 A simplified schematic of the TiO2 photocatalysis process..... 5

Figure 3.1 Schematic diagram of equipment set up for electrospinning of PAN/TiO2 nanofibers..... 26

Figure 3.2 Calibration curve Cr(VI) Standard solution 28

Figure 3.3 Experimental set up used to test photocatalytic reduction of Cr(VI) 30

Figure 4.1.1 SEM images of the TiO2/PAN nanofibers 34

Figure 4.2.1 Kinetic of adsorption of Cr(VI) on TiO_2/PAN nanofobers at different pHs. 38

Figure 4.3.1 Variation of reaction system temperature..... 39

Figure 4.3.2 The Cr(VI) reduction measurements with the initial concentration of 5mg/L(100µM) at different pH conditions under the UV+Visible light within 400min exposure. 40

Figure 4.3.3 The Cr(VI) reduction measurements with the initial concentration of 5mg/L(100µM) at pH of 7and 8.5 under the UV+Visible light within 2 day (2880 min) exposure. 41

Figure 4.3.4 The pseudo-first order kinetics plots for Cr(VI) catalytic reduction at pH of 2.5, 5 (a) 7, 8.5 (b) under UV+visible light. 42

Figure 4.3.5 The recovered TiO_2/PAN nanofibers performance of Cr(VI) photocatalysitc reduction. 44

Figure 4.3.6 SEM images of the recovered TiO_2/PAN nanofibers at pH of 7..... 45

Figure 4.3.7 The Cr(VI) reduction measurements with the initial concentration of 5mg/L(100µM) at pH of 2.5 and 5 under the different light source..... 47

Figure 4.3.8 The Cr(VI) reduction measurements with the initial concentration of 5mg/L at pH of 7 under different light source..... 47

Figure 4.3.9 The Cr(VI) reduction measurements with the initial concentration of 5mg/L at pH of 8.5 under different light source..... 48

Figure 4.3.10 The pseudo-first order kinetics plots for Cr(VI) catalytic reduction at pH of 2.5, 5 (a) 7, 8.5 (b) under visible light. 49

Figure 4.3.11 Control test for Cr(VI) reduction in presence of HA in dark with catalyst and under UV+visible light without catalyst, pH=7, [HA] =2 mg/L. 51

Figure 4.3.12 Effect of HA on Cr(VI) removal under UV+visible light (a) pH=2.5 (b) pH=7 52

Figure. 4.3.13 The pseudo-first order kinetics plots for Cr(VI) catalytic reduction at pH of 2.5 and 7 under UV+visible light. Effect of HA on the removal of Cr(VI). 53

Figure 4.3.14 UV-vis absorbance of humic acid 54

Figure 4.3.15 Effect of HA on Cr(VI) removal under visible light, pH=7. 55

Figure 4.3.16 The pseudo-first order kinetics plots for Cr(VI) catalytic reduction at pH 7 under visible light. Effect of HA on the removal of Cr(VI). 56

LIST OF TABLES

Table Page

Table 2.1 The BET specific surface area of different electrospun anatase-phase TiO2 nanofibers..... 11

Table 4.3.1 Rate constants at various pHs 42

Table 4.3.2 kinetic parameters summary 48

Table 4.3.3 kinetic parameters summary 54

Chapter 1 INTRODUCTION

The rapid development of civilization and industrial activities has led to a series of environmental problems. For decades, large amount of pollutants have been discharged into the environment intentionally or accidentally, including toxic metals in water with a great health concern. Cadmium, zinc, copper, nickel, lead, mercury and chromium are often detected in industrial wastewaters, generated from metal plating, mining, smelting, battery manufacture, tanneries, petroleum refining, paint manufacture, pesticides, pigment manufacture, printing and photographic industries, etc. (Wan Ngah and Hanafiah 2008). Different from the organic components, toxic metallic ions generally are not degradable and have an infinite lifetime, thus they may be accumulated in living tissues, causing various diseases and environmental problems. Some of the metal irons are actually necessary for human body in trace amounts while others are carcinogenic or toxic, damaging the nervous system, kidney, liver, skin, bones, or teeth. The removal of toxic metals in an effective and economic way has been a critical issue for the environment improvement.

Chromium is a heavy metal, naturally found in rocks and minerals, animals, and plants, with multiple applications in industry. In aquatic environments, chromium exists mostly in the hexavalent chromium (Cr(VI)) and trivalent chromium (Cr(III) states. Anionic Cr(VI) is far more mobile and toxic than Cr(III) and more difficult to remove from water. Similar to many other metal cations, however, aqueous Cr(III) can be readily precipitated as $Cr(OH)_3$ or removed by adsorption and ion exchange. Thus, reduction of chromium from its hexavalent to trivalent states simplifies its removal from effluent and also reduces its toxicity and mobility.

Chemical precipitation has traditionally been the most used method for the treatment of Cr(VI) following its reduction. The most widely-used industrial reducing agents are sulfur dioxide gas or sodium bisulfite in an acid solution. Both of these reactants form the same active reducing agent, which is sulfurous acid. Since Cr(III) hydroxide is precipitated, the resulting effluent will contain little or no residual chromium. One of the main problems of using this technique is that large amounts of residual sludge are generated. The sludge is difficult to manage, transport, and dispose, and there are associated costs with each step (Barrera-Díaz, Lugo-Lugo et al. 2012). Thus, development of new technologies is needed to address these problems.

Photocatalytic technology has been studied since 1970s and widely explored for the degradation of organic and inorganic contaminants in the presence of certain semiconductors under light exposure. Much research in the literature has been focused on understanding the mechanism or enhancing the efficiency of the photocatalytic process especially for water pollution treatment. The major advantages of this technology are (Kabra, Chaudhary et al. 2004):

(i) Photocatalysis provides a good substitute for the energy-intensive conventional treatment methods with the capacity for using renewable and pollution-free solar energy;

(ii) The photocatalytic reaction conditions are mild, and a lesser chemical input is required;

(iii) Secondary waste generation is minimal.

With these advantages, we expect that the photocatalysis process be suitable for the treatment of drinking water and industrial wastewater in a large scale for its efficiency, security and energy conservation.

The photocatalytic reduction of Cr(VI) to Cr(III) by some semiconductors under UV/visible light illumination has been reported in 1979 (Yoneyama, Yamashita et al. 1979), titanium dioxide nanomaterial has attracted a worldwide attention and been considered as a simple, inexpensive and effective photocatalyst. However, pure TiO_2 can only be activated by the ultra-violet light irradiation due to its high energy band gap, and there is only less than 10% of the natural light energy could be harvested by normal TiO_2. As a result, much effort has been made to modify TiO_2 nanomaterial so as to improve its photocatalytic activity with visible light. TiO_2 nanomaterials doped with the element such as nitrogen, carbon, sulfur, vanadium, and lanthanum are found capable of absorbing and being activated by visible light (Asahi, Morikawa et al. 2001, Yu, Yu et al. 2007).

To promote the catalytic application of TiO_2 under the visible light, there is a need to manufacture the TiO_2 nanomaterial through a mild and simple process. TiO_2 nanomaterial with 1- dimensional nano structure such as nanofiber was successfully fabricated via a high yield and low cost electrospinning process (Li and Xia 2003), an approach widely used for producing nano-structured materials. It is also known that some functional groups (Hydroxy, Cyano, Carboxyl, etc.) in the nanofiber structure can interact with metal ions. Especially, nitrogen and carbon of polyacrylonitrile (PAN), a common, cheap and nontoxic polymer material used for electrospinning, can be potentially doped into TiO_2 nanofibers (Im, Kim et al. 2008, Nguyen and Deng 2012, Zhang, Li et al. 2012).

The goal of this study, therefore, is to investigate the catalysis of the PAN/TiO_2 nanofibers, developed and prepared by Nguyen and Deng (Nguyen and Deng 2012), on the reductive degradation of Cr(VI) under the visible light sources. The effects of various parameters such as pH and reaction concentrations were evaluated in the research.

This thesis includes 5 chapters. Chapter 1 here is the introduction, which gives a brief background on both photocatalytic technique and degradation of Cr(VI). A more detailed literature review related to this research is presented in chapter 2, including the basic mechanism of photocatalytic process, preparations and modifications of TiO_2, electrospinning technique and treatment technology of Cr(VI). In chapter 3, the methodology of this research is introduced, including the determination of Cr(VI), data processing and model application. Details about the preparation process of TiO_2/PAN nanofibers and Cr(VI) reduction experiment are also described in this chapter. Chapter 4 presents the experimental results under various conditions on Cr(VI) photocatalytic degradation as well as the characterization data of TiO_2/PAN nanofibers. Chapter 5 summarizes the main conclusions for the whole research, perspectives obtained from this study, and recommendations for possible future work.

Chapter 2 BACKGROUND AND LITERATURE REVIEW

2.1 TiO_2 and photocatalysis process

2.1.1 Basic mechanism of photocatalysis

Photocatalysis involves capturing of photons by a semiconductor such as titanium dioxide (TiO2), resulting in the creation of electrons and positive holes and subsequent redox reactions (Figure 2.1).

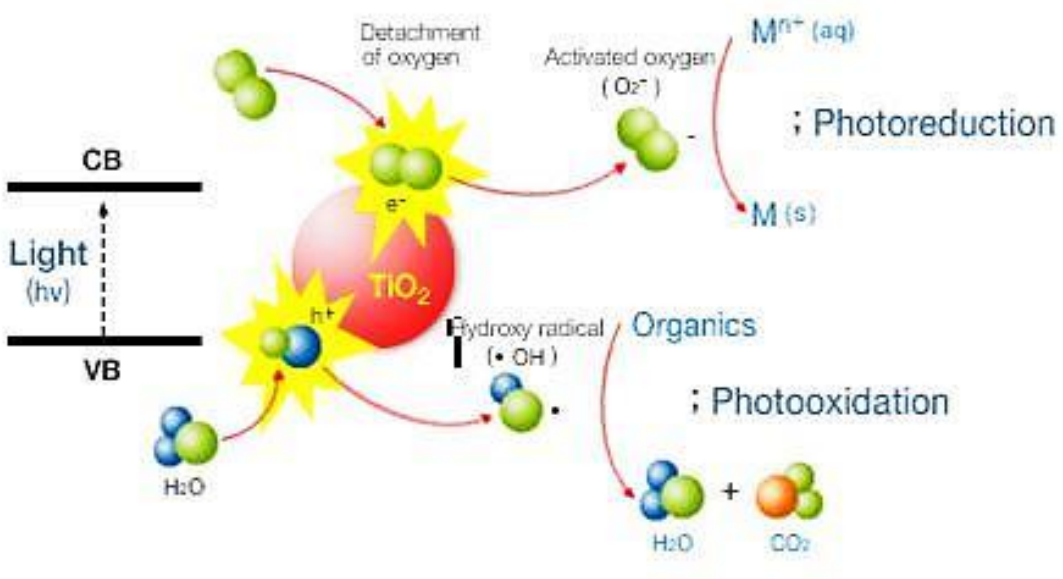

Figure 2.1 A simplified schematic of the TiO2 photocatalysis process

(http://www.davidonindustries.com/page.php/id/151)

More specifically, the void energy region where no electron states can exist in a semiconductor is called the band gap. The band gap also refers to the energy difference

between the top of the filled valence band and the bottom of the vacant conduction band (Linsebigler, Lu et al. 1995). When a semiconductor is exposed to photon, the electron present in the valence band jumps to the conduction band if the photon energy ($h\upsilon$) equals or exceeds the band gap energy of the semiconductor/photocatalyst. As the result, an electron vacancy or a positive charge called a hole (h+) is generated in the valence band (Kabra, Chaudhary et al. 2004).

$$h\nu + \text{semiconductor} \rightarrow h^+ + e^-$$

Ultimately, the process creates a reaction between the activated electrons or the generated holes and the chemicals adsorbed on the surface of the semiconductor. Generally, the hole oxidizes water to hydroxyl radicals which subsequently initiate a chain of reactions leading to the oxidation of organics. Similarly, the electron can be donated to an electron acceptor such as a metal ion (with a reduction potential more positive than the band gap of the photocatalyst). This metal ion can be reduced to its lower valence states and deposited on the surface of the photocatalyst/semiconductor (Kabra, Chaudhary et al. 2004). The recombination of the electron and the hole must be prevented as much as possible to increase the photocatalytic reaction efficiency. Among the semiconductors capable of photocatalysis, titanium dioxide (TiO_2) is the most widely used because it is photostable, chemically stable, photoactive, relatively inexpensive, and non-toxic.

2.1.2 TiO_2 nanofiber and its modification

The photocatalytic properties of titanium dioxide were discovered by Akira Fujishima in 1967 and published in 1972. Their work stimulated the rapid development of

photocatalysis for a wide range of environmental and energy applications. With the high oxidation potential of the positive hole and hydroxyl radicals, the photocatalytic process induced by semiconductor such as TiO_2 is capable of oxidizing a wide range of contaminants in water and air.

The use of nano-structured materials may lead to improved photocatalytic efficiencies, since the reduction in particle size could result in a greater surface area and possibly size quantization effects. Many investigations have found that TiO_2 is much more effective as a photocatalyst in the form of nanostructure than in bulk powder. Recently, TiO_2 with nanostructure has been prepared in the form of particles, crystals, thin films, tubes and fibers. TiO_2 nanoparticles have been commonly used for research and manufactured at an industrial scale today. However TiO_2 nanoparticles have some disadvantages in applications for water treatment, for example, an extra separation step is necessary for its removal from the reaction system. Therefore, it is meaningful to have other structures of TiO_2 nanomaterial to improve its applicability. Nanofiber is a common form of 1-dimensional nanomaterial. It has been successfully prepared by the electrospinning technology which is considered as simple and versatile in fiber preparation (Greiner and Wendorff 2007). As a heterogeneous photocatalyst, TiO_2 nanofiber not only has a large surface area but also the characteristic provided by 1-dementional structure, notably, it can be prepared with fixed supporting substrates in the form of thin film or mat. Because of the latter feature, TiO_2 nanofiber has the advantage of being easily separated following its use as a catalyst in water.

The ultraviolet light (UV) is a kind of electromagnetic radiation with a wavelength ranging from 400 nm and 100 nm, corresponding to photon energies from 3 eV to 12.4 eV. At the ground level, total sunlight power is composed of 44% visible light, 53% infrared and 3% ultraviolet. A considerable portion of UV is blocked by earth's air and ozone layer. The band gap of bulk TiO_2 is 3.0 eV for rutile and 3.2 eV for anatase (Linsebigler, Lu et al. 1995, Yu, Yu et al. 2007), which means the pure TiO_2 can only be activated by the UV light. Modification and doping of TiO_2 to enlarge the range of light wavelength to get photoactivity with visible lights has been an active area of research (Anpo 2000). Various metallic and non-metallic dopants have been found to cause shift in the absorption band towards visible light region especially for metal ions such as V, Cr, Mn, Fe and Ni. Stimulated by the report of Asahi et al. in 2001, there has been an explosion of interest in TiO_2 doping with non-metal ions (e.g. N, C, S, F) recently (Di Valentin, Finazzi et al. 2007).

Nitrogen is considered as one of the most effective non-metal ion dopants for TiO_2. Optical absorption of the N-doped TiO_2 was significantly enhanced in the visible light region with a wavelength less than 500 nm comparing to the original TiO_2. Improvement on photocatalytic efficiency was also observed in the degradation of various contaminants under visible light irradiation. The N-doped TiO_2 materials were first prepared by sputtering TiO_2 anatase powder in nitrogen/argon gas mixture and annealed at 550^oC for 4 hours (Asahi, Morikawa et al. 2001). Similarly, carbon doped (C-doped) TiO_2 nanomaterial has been prepared usually by heating TiO_2 nanomaterial with activated carbon and carbon nanotube (Chen and Mao 2007), or processing TiO_2 nanomaterial in pure methane (CH_4) surrounding.

However, the commonly-used nitrogen and carbon doping method cannot be directly applied on 1-dimension nanomaterial like TiO_2 nanofiber. These methods require heating the material in the surrounding of dopant at high temperature, which often destroy the nanofiber structures supported by polymer substrates and result in materials with a low mechanic strength (Kim, Cho et al. 2010). Once the TiO_2 nanofiber becomes fragile and easily-broken in applications, the advantage of the nanofiber will no longer exist over the nanoparticle. According to the previous investigation in Deng's research group (Nguyen and Deng 2012), a reliable doping method for TiO_2 nanofibers is followed in this research. Nitrogen or carbon doped TiO_2 nanofibers were prepared by the thermal resistant polymer PAN containing carbon and nitrogen as fiber substrate for electrospinning and annealing process. These TiO_2 nanofibers were used as the photocatalyst for the degradation of Cr(VI) at different reaction conditions and under various light source irradiations.

2.2 Electrospinning technique

Electrospinning uses an electrical charge to create very fine (typically on the micro or nano scale) fibers from a liquid. The electrospinning technique was first developed for the synthesis of nanofibers since 1934 (Huang, Zhang et al. 2003). It is a process in which a strong electrostatic force created by a high static voltage is applied to a polymer solution placed into a container with a millimeter diameter nozzle. When the body of the liquid becomes charged, and electrostatic repulsion counteracts the surface tension, the droplet is stretched and ejected from the nozzle. The combination of electrostatic repulsion and the surface tension will result in the formation of the well-known Taylor cone. After the solvents evaporate during the course of jet spraying, the nanofibers are collected on a

grounded collector. In some experiments, the fixed metal foil is replaced by a constantly rotating drum for the purpose of achieving better distribution of nanofibers deposited on the collector surface (Chandrasekar, Zhang et al. 2009). The elongation and thinning of the fiber leads to the formation of uniform fibers with nanometer-scale diameters. Electrospinning shares characteristics of both electrospraying and conventional solution dry spinning of fibers (Ziabicki 1976). The process does not require the usage of coagulation chemistry or high temperatures to produce solid threads from solution. This makes the process particularly suitable for the production of fibers with large and complex molecules.

In the recent decade, there have been numerous researches devoted to preparations and characterizations of structures and properties of electrospun TiO_2 nanofibers. In general, these nanofibers are made by electrospinning spin dopes containing TiO_2 under amorphous form as precursors other than using crystalized TiO_2 directly, followed by annealing the as-electrospun precursor nanofibers at high temperature > 500^oC, which converts the precursor into crystallized forms of anatase and rutile exhibiting photocatalytic effects. TiO_2 nanofibers have been prepared by electrospinning processes with Ti precursors such as titanium isopropoxide (Li and Xia 2003). Moreover, titanium dioxide nanoparticles (P25 Degussa) (Im, Kim et al. 2008, Shaham Waldmann and Paz 2010) have been directly applied to TiO_2 nanofibers fabrication in some research papers currently.

It is well-known that the photocatalytic activity of TiO_2 is strongly dependent on the specific surface area and morphological structure of anatase-phase TiO_2. Various

preparation methods and precursors result in various morphological structures and specific surface areas. Table 2.1 illustrated the BET specific surface area of different electrospun anatase-phase TiO_2 nanofibers according to the latest study (He, Cai et al. 2013).

Table 2.1 The BET specific surface area of different electrospun anatase-phase TiO2 nanofibers.

Sample	BET specific surface area (m2/g)
Solid TiO_2 nanofibers	15.2
Hollow/tubular TiO_2 nanofibers	27.3
Porous TiO_2 nanofibers made from the precursor of Al_2O_3/TiO_2 composite nanofibers	106.5
Porous TiO_2 nanofibers made from the precursor of ZnO/TiO_2 composite nanofibers	148.6

In Nguyen and Deng's research, they enhanced the mechanical properties of prepared TiO_2 nanofibers and modify them with carbon and nitrogen as dopants in order to achieve activation under visible lights and improve the photocatalytic efficiency via a new preparation method.

In this research, I followed the preparation method of TiO_2/PAN nanofibers developed by Nguyen and Deng (2012) and continued their investigation to apply the nanofibers on the photocatalytic degradation of Cr(VI). The practical application of the TiO_2/PAN nanofibers for Cr(VI) treatment in liquid phase was tested at different reaction conditions.

2.3 Degradation of Hexavalent Chromium

Chromium is naturally found in rocks, soil, and volcanic dust and gases. It comes in various forms including trivalent chromium and hexavalent chromium. Hexavalent chromium(Cr(VI)), as a frequent contaminant in waste waters, is widely used for the production of stainless steel, textile dyes, wood preservation, leather tanning, and as anti-corrosion and conversion coatings as well as a variety of niche uses. Cr(VI) is pproximately 10 to 100 times more toxic than Cr(III). The USEPA (United States Environmental Protection Agency) classifies Cr(VI) as a known human carcinogen via inhalation. As a common metallic contaminant, Cr(VI) has been listed as the heavy metals of highest concern by the European community.

The most probable Cr(VI) species in aqueous solution are Cr_2O7^{2-} , CrO_4^{2-} , H_2CrO_4, and $HCrO^{4-}$, the relative distribution of which depends on the solution pH, the Cr(VI) concentration and the redox potential (Cespón-Romero, Yebra-Biurrun et al. 1996). However, none of these Cr(VI) species form insoluble precipitates, which makes separation through a direct precipitation process impossible. Like many metal ions, Cr(III) forms insoluble precipitates. Thus, reducing Cr(VI) to Cr(III) simplifies its removal from effluent and also reduces its toxicity and mobility (Barrera-Díaz, Lugo-Lugo et al. 2012).

2.3.1 Cr(VI) in drinking water

Chromium can affect water source naturally, or through contamination discharged from industrial and landfill waste streams. Exposure in the drinking water is the dominant way for hexavalent chromium to affect public health. A study conducted by the National

Toxicology Program (NTP) published in 2007 concluded that hexavalent chromium is carcinogenic when ingested in drinking water (EPA 2011). Therefore, official institutions have begun to investigate the feasible methods to reduce the concentration of Cr(VI) in drinking water.

The current US national drinking water standard, or maximum contaminant load (MCL), for total chromium is 100 micrograms per liter, or parts per billion (ppb). Total chromium is the combined concentration of all states of chromium, including hexavalent chromium and the less toxic trivalent chromium. Some states have stricter standards such as California, which adopts the standard of 50 ppb for total chromium. There is currently no drinking water limit established by the USEPA specifically for Cr(VI). As of 2010, the California EPA had proposed a goal of 0.2 parts per billion for Cr(VI). A final Public Health Goal of 0.02 ppb was established in July 2011 (Hexavalent Chromium PHG).

Cr(VI) is among the 20 chemical that being reviewed by USEPA for further regulation recently. In 2011, the USEPA issued a risk assessment of hexavalent chromium which emphasizes the health risk of Cr(VI) from drinking water. It is probable that a stricter US national standard for hexavalent chromium will be established because of the assessment. Not only the standard, the feasibility and costs of removing hexavalent chromium from drinking water is also taken into consideration and focused by the regulators.

2.3.2 Traditional treatment method for Cr(VI)

For the treatment of chromate-containing rinse water, the typical procedure is the reduction of hexavalent chromium to its trivalent state, followed by its precipitation as Cr(III) hydroxide. The most common industrial reducing agents are sulfur dioxide gas or sodium bisulfite in an acid solution. Sulfur dioxide gas usage is mostly restricted to large scale treatment plants and sodium bisulfite is used at the small and medium-sized systems, but it is sometime also used at large systems. Both of these reactants form the same active reducing agent, sulfurous acid. The reactions between Cr(VI) and sodium bisulfite or sulfur dioxide are shown as follow (Barrera-Diaz, Lugo-Lugo et al. 2012).

$$4CrO_4^{2-}\,(aq) + 6NaHSO_3\,(aq) + 3H_2SO_4\,(aq) + 8H^+\,(aq) \rightarrow$$

$$2Cr_2(SO4)_3\,(aq) + 3Na_2SO_4\,(aq) + 10H_2O \qquad (2.1)$$

$$2CrO_4^{2-}(aq) + 3SO_2(g) + 4H^+(aq) \rightarrow Cr_2(SO_4)_3(aq) + 2H_2O \qquad (2.2)$$

Precipitation of Cr(III) by sodium hydroxide is indicated in reaction (2.3). Since Cr(III) hydroxide is precipitated, the ultimate effluent will contain no residual or only trace amount of chromium.

$$Cr_2(SO_4)_3\,(aq) + 6NaOH\,(aq) \rightarrow 2Cr(OH)_3\,(s) + 3Na_2SO_4\,(aq) \qquad (2.3)$$

The reduction efficiency of the reaction is highly dependent on pH. Conventional processes are operated at pH 2.0 to 3.0. Sulfuric acid usually should be added into the solution to reduce the pH because most of the feeding waste stream is above the optimal operation pH level. This is a drawback of the reaction process with sodium bisulfite as

reducing agent since the following metal removal step performed by precipitation with alkali (pH equals 7.0 to 9.5) is necessary, and therefore the addition of acid increases the need of alkali reagent.

Due to the lower chemical cost, sulfur dioxide gas is the choice of reducing agent for larger systems. However, the limitation of it for the smaller scale is that a more expensive chemical feed system is required. Furthermore, sulfur dioxide is a kind of toxic gas. To overcome the health problem, a vacuum system is usually installed to prevent the leak of sulfur dioxide to the working area, which increases the capital cost of using this reagent as well.

Other reducing agent in common use is ferrous sulfate which is applied in an acid environment for a number of years. When ferrous sulfate is used as the agent, large amount of ferric hydroxide is produced as a solid waste owing to the precipitation of ferric hydroxide in the neutralization phase of the treatment, requiring subsequent disposal.

Overall, the conventional treatment method of redox reaction all requires additional pre- or post- treatment process. Considerable residual sludge is generated when using this technique, and there are associated cost and challenges for managing, transporting and final disposal of these wastes. Therefore, new technologies are being developed to better treat Cr(VI) contamination.

Electrochemical methods, ion exchange, ultrafiltration, flotation, adsorption and photocatalysis come up in succession. Among these techniques, photocatalysis has long

been applied to treat organic and inorganic contaminants because of its many advantages mentioned previously.

2.3.3 Photocatalytic reduction of Cr(VI)

The photocatalytic reduction of Cr(VI) to Cr(III) over some semiconductors under UV/visible light illumination was reported since 1979 (Yoneyama, Yamashita et al. 1979). The utilization of solar light for photocatalytic degradation was investigated on the modified TiO_2 in recent decades. The photocatalytic reduction of Cr(VI) by TiO_2 in both the absence and presence of organic compounds has been studied for its application to the oxidation of organic compounds and the reduction of metal ions. The overall reaction of Cr(VI) degradation is proposed as below (Khalil, Mourad et al. 1998):

$$2Cr_2O_7^{2-} + 16H^+ \rightarrow 4Cr^{3+} + 8H_2O + 3O_2 \quad (2.4)$$

Various factors that act as the reaction parameters have been studied in the related research papers. The reaction kinetic and the photocatalytic efficiency are strongly affected by some of these parameters.

- **pH**

Research has proven that the photocatalysis reaction of Cr(VI) degradation is highly pH sensitive. Most papers conclude that Cr(VI) reduction rate decreased with increasing pH and was efficient at pH below 3, forming Cr(III) in the solution. The relatively large change in reduction rate between pH 3 and pH 4 is probably related to pH-dependent variations in surface or substrate interactions and a shift from the dichromate anion to chromate (Prairie, Evans et al. 1993). The reaction efficiency was significantly greater at

acidic pH than at neutral pH. At pH higher than 4, Cr(III) formed a stable precipitate on the catalyst (Prairie, Evans et al. 1993). Supporting view by other research also indicated that fouling of the photocatalyst happened at pH above 4 (Giménez, Aguado et al. 1996). The thermodynamic study of Cr(VI) photoreduction by TiO_2 at pH from 0 to 10 in aqueous media was discussed. Lin and Wei et al. concluded that the thermodynamic driving force for Cr(VI) reduction on TiO_2 in basic aqueous solutions was less than that in acidic media (Lin, Wei et al. 1993).

- **Light intensity**

As the photon-induced reaction, the photocatalytic reaction of Cr(VI) is strongly affected by the light intensity. The photocatalytic reduction rate of Cr(VI) was found to be linearly increased with light intensity until certain optimum light intensity was reached, possibly because the light intensity is too excessive in comparison with the amount of TiO_2 particles presented in solution to activate extra electrons and holes on the surface of TiO_2 particles. (Ku and Jung 2001).

- **Photocatalyst dosage**

In the early research, the amount of the photocatalyst added in the reaction solution has already been investigated. In general, the removal of Cr(VI) and reaction rate increases with increasing catalyst dosage. It is noteworthy that much literature shows that there is an optimal value for the catalyst dosage. Ku and Jung (2001) reported that reduction rate constants of Cr(VI) seemed to gradually approach a limiting value for higher dosages of TiO_2. The removal efficiency is more likely decreased if the dosage is beyond this value.

This result is not only for TiO_2 as photocatalyst or degradation of Cr(VI) but also has been supported by many other papers since the very beginning of the photacatalysis study. Reiche et al.(1979) observed the similar experimental result for the photoreduction of Cu(II) by UV/TiO_2, while Wang et al. (1992) also reported that for the reduction of Cr(VI) via UV/CdS photocatalytic process, the optimum CdS dosage was about 5 g/l, and as a matter of fact, excess amounts of CdS would gradually decrease the Cr(VI) reduction rate (Ku and Jung 2001). This can be explained from the mixed results of various effects with increasing the catalyst dosage. As positive effects, the adsorption sites on the catalyst, as well as the generation of free electrons in the conduction band, should increase with larger dosage. The decrease of UV light penetration caused by the suspensions of photocatalyst particles could be the very possible explanation as the negative effect (Yang and Lee 2006).

- **Presence of organic compounds**

The ability of semiconductor for oxidation of organic compounds and reduction of metal ions has already been verified many years ago. In order to figure out that if the photocatalysis technology for water treatment is suitable for the practical condition, research was carried out to investigate the effect of organic materials on the photocatalytic reduction of Cr(VI). Result shows that with the presence of both the organic compounds (such as humic acid, oxalate, ethylenediaminetetraacetic acid, nitrilotriacetic acid and phenol) and Cr(VI) in the reaction system, the reduction rate for both organic and inorganic components increase to some degree (Prairie, Evans et al. 1993). The photocatalytic reduction of Cr(VI) accompany with the photocatalytic oxidation of the added organics,

leading to a promotion of the photocatalytic reduction of Cr(VI), is due to the significant synergistic effect between Cr(VI) and organic contaminants (Wang, Wang et al. 2008).

Organic matter supplies electrons to the photocatalytic system and may act as a scavenger of positive holes in the valence band of the photocatalyst. Even though the adsorption of Cr(VI) onto catalyst surface could be obstructed by the organics, enhanced photocatalytic efficiencies and reduction rate resulted from the reduced recombination between the positive holes and electrons might compensate for the negative effect on the removal of Cr(VI) (Yang and Lee 2006).

However, similar to the effect of photocatalyst dosage to the reaction, there was an optimal value for the organic compounds for the acceleration of Cr(VI) reduction. Reduction rate inhibition was observed at an organic concentration beyond a certain limit. It is probably because that organic compounds at high concentration absorbs the UV light so strongly and acts as an internal filter (Lin, Wei et al. 1993). The effect on Cr(VI) reduction depends on specific organic compounds. The systems with low molecular weight acids, alcohols, and aldehydes produced reduction rates very similar to those observed without organics. In contrast, the systems with EDTA, salicylic acid, and citric acid all produced rapid reduction of Cr(VI) (Lin, Wei et al. 1993).

- **Nanotechnology**

The rapid development of nanotechnology has resulted in many materials with novel functionalities that are potententially useful for environmental protection applications. For example, TiO_2 nanoparticles and nanofibers has resulted in an enhanced

catalytic activity for photocatalytic Cr(VI) reduction and the materials with hydrothermal post treatment exhibited the highest catalytic activity among TiO_2 nanoparticles (Mu, Xu et al. 2010). Electrospinning technology has been successfully applied to the preparation of the nano- to sub-micrometre fibers. Electrospun polymeric nanofibers containing both carbon nanotubes and titanium dioxide particles were generated a few years ago. The nanofibers consisted of polymer nanofibrous matrix, carbon nanotubes and embedded Degussa P25 TiO_2 particles has been applied to Cr(VI) photoreduction. About 86% of Cr(VI) were reduced after 2 hours irradiation under UV light at pH of 2 (Shaham Waldmann and Paz 2010). Electrophoretic deposition (EPD) has been proposed as a versatile and low cost alternative procedure to deposit TiO_2 in dense layers onto electrodes to be used in photocatalytic degradation of Cr(VI) (Pifferi, Spadavecchia et al. 2013). Kajitvichyanukul et al. found that differences in photocatalytic reduction rate of Cr(VI) could be correlated with the structural morphology and composition of the TiO_2 nanofilm at different heating temperatures and coating cycles (Kajitvichyanukul and Amornchat 2005).

In our research, the pH of reaction system, light source and presence of organic were taken as the parameter for the study of the Cr(VI) photocatalytic degradation. The results of our research matched the conclusion of the literature review as mentioned above on the whole.

Reference

http://switchboard.nrdc.org/blogs/gsolomon/california_finally_takes_leade.html

http://www.oehha.org/water/phg/072911Cr6PHG.html

http://www.nmfrc.org/bluebook/sec622.htm

Anpo, M. (2000). "Utilization of TiO2 photocatalysts in green chemistry." Pure and Applied Chemistry **72**(7): 1265-1270.

Asahi, R., et al. (2001). "Visible-light photocatalysis in nitrogen-doped titanium oxides." Science **293**(5528): 269-271.

Barrera-Diaz, C. E., et al. (2012). "A review of chemical, electrochemical and biological methods for aqueous Cr(VI) reduction." J Hazard Mater **223-224**: 1-12.

Barrera-Díaz, C. E., et al. (2012). "A review of chemical, electrochemical and biological methods for aqueous Cr(VI) reduction." Journal of Hazardous Materials **223-224**: 1-12.

Cespón-Romero, R. M., et al. (1996). "Preconcentration and speciation of chromium by the determination of total chromium and chromium(III) in natural waters by flame atomic absorption spectrometry with a chelating ion-exchange flow injection system." Analytica Chimica Acta **327**(1): 37-45.

Chandrasekar, R., et al. (2009). "Fabrication and characterization of electrospun titania nanofibers." Journal of Materials Science **44**(5): 1198-1205.

Chen, X. and S. S. Mao (2007). "Titanium dioxide nanomaterials: Synthesis, properties, modifications and applications." Chemical Reviews **107**(7): 2891-2959.

Di Valentin, C., et al. (2007). "N-doped TiO2: Theory and experiment." Chemical Physics **339**(1-3): 44-56.

EPA (2011). "EPA's recommendations for enhanced monitoring for Hexavalent Chromium (Chromium-6) in Drinking Water." **Retrieved**

Giménez, J., et al. (1996). "Photocatalytic reduction of chromium(VI) with titania powders in a flow system. Kinetics and catalyst activity." Journal of Molecular Catalysis A: Chemical **105**(1-2): 67-78.

Greiner, A. and J. H. Wendorff (2007). "Electrospinning: A fascinating method for the preparation of ultrathin fibers." Angewandte Chemie - International Edition **46**(30): 5670-5703.

He, G., et al. (2013). "Electrospun anatase-phase TiO2 nanofibers with different morphological structures and specific surface areas." Journal of Colloid and Interface Science **398**: 103-111.

Im, J. S., et al. (2008). "Preparation of PAN-based electrospun nanofiber webs containing TiO2 for photocatalytic degradation." Materials Letters **62**(21-22): 3652-3655.

Kabra, K., et al. (2004). "Treatment of hazardous organic and inorganic compounds through aqueous-phase photocatalysis: A review." Industrial and Engineering Chemistry Research **43**(24): 7683-7696.

Kajitvichyanukul, P. and P. Amornchat (2005). "Effects of diethylene glycol on TiO2 thin film properties prepared by sol-gel process." Science and Technology of Advanced Materials **6**(3-4 SPEC. ISS.): 344-347.

Khalil, L. B., et al. (1998). "Photocatalytic reduction of environmental pollutant Cr(VI) over some semiconductors under UV/visible light illumination." Applied Catalysis B: Environmental **17**(3): 267-273.

Kim, Y. B., et al. (2010). "Fabrication and characterization of TiO2/poly(dimethyl siloxane) composite fibers with thermal and mechanical stability." Journal of Applied Polymer Science **116**(1): 449-454.

Ku, Y. and I.-L. Jung (2001). "Photocatalytic reduction of Cr(VI) in aqueous solutions by UV irradiation with the presence of titanium dioxide." Water Research **35**(1): 135-142.

Li, D. and Y. Xia (2003). "Fabrication of titania nanofibers by electrospinning." Nano Letters **3**(4): 555-560.

Lin, W.-Y., et al. (1993). "Photocatalytic reduction and immobilization of hexavalent chromium at titanium dioxide in aqueous basic media." Journal of the Electrochemical Society **140**(9): 2477-2482.

Linsebigler, A. L., et al. (1995). "Photocatalysis on TiO2 surfaces: Principles, mechanisms, and selected results." Chemical Reviews **95**(3): 735-758.

Mu, R., et al. (2010). "On the photocatalytic properties of elongated TiO2 nanoparticles for phenol degradation and Cr(VI) reduction." Journal of Hazardous Materials **176**(1-3): 495-502.

Nguyen, H. Q. and B. Deng (2012). "Electrospinning and in situ nitrogen doping of TiO2/PAN nanofibers with photocatalytic activation in visible lights." Materials Letters **82**(0): 102-104.

Pifferi, V., et al. (2013). "Electrodeposited nano-titania films for photocatalytic Cr(VI) reduction." Catalysis Today **209**: 8-12.

Prairie, M. R., et al. (1993). "An investigation of TiO2 photocatalysis for the treatment of water contaminated with metals and organic chemicals." Environmental Science and Technology **27**(9): 1776-1782.

Shaham Waldmann, N. and Y. Paz (2010). "Photocatalytic reduction of cr(VI) by titanium dioxide coupled to functionalized cnts: An example of counterproductive charge separation." Journal of Physical Chemistry C **114**(44): 18946-18952.

Wan Ngah, W. S. and M. A. K. M. Hanafiah (2008). "Removal of heavy metal ions from wastewater by chemically modified plant wastes as adsorbents: A review." Bioresource Technology **99**(10): 3935-3948.

Wang, L., et al. (2008). "Photocatalytic reduction of Cr(VI) over different TiO2 photocatalysts and the effects of dissolved organic species." Journal of Hazardous Materials **152**(1): 93-99.

Yang, J. K. and S. M. Lee (2006). "Removal of Cr(VI) and humic acid by using TiO2 photocatalysis." Chemosphere **63**(10): 1677-1684.

Yoneyama, H., et al. (1979). "Heterogeneous photocatalytic reduction of dichromate on n-type semiconductor catalysts [5]." Nature **282**(5741): 817-818.

Yu, H., et al. (2007). "Photocatalytic activity of the calcined H-titanate nanowires for photocatalytic oxidation of acetone in air." Chemosphere **66**(11): 2050-2057.

Zhang, C., et al. (2012). "Polyacrylonitrile/manganese acetate composite nanofibers and their catalysis performance on chromium (VI) reduction by oxalic acid." J Hazard Mater **229-230**: 439-445.

Ziabicki, A. (1976). Fundamentals of fibre formation: the science of fibre spinning and drawing.

Chapter 3 EXPERIMENTAL PROCEDURE AND METHODOLOGY

Overview

The materials and experimental procedure are presented in this chapter, including those related to preparation of TiO_2/PAN nanofiber and removal of Cr(VI) from water. Section 3.1 summarizes the materials and equipment used. In section 3.2, the preparation steps of TiO_2/PAN nanofibers by the widely known electrospinning technique are described in detail. Section 3.3 shows the procedure for Cr(VI) analysis, and Section 3.4 describes the process of measuring Cr(VI) sorption onto the TiO_2/PAN nanofibers mat and characterizing the photocatalytic reduction kinetics of Cr(VI) under different pH and concentration conditions. Section 3.5 is on the data processing and modeling.

3.1 Materials and equipment

Titanium (IV) isopropoxide (TIIP, CAS 546-68-9), acetone (CAS 67-64-1), humic acid (CAS 1415-93-6) and 1-5 diphenylcarbazide (CAS 140-22-7) were purchased from Sigma Aldrich (St Louis, Missouri). Polyacrylonitrile (PAN, CAS 250014-41-9, MW= 150,000) was purchased from Scientific Polymer Production Inc. (Ontario, New York). Dimethyl sulfoxide (DMSO, CAS 67-68-5) were purchased from Fisher Scientific (Fairlawn, New Jersey). The stock Cr(VI) solution was prepared by the standard Cr(VI) solution (potassium dichromate, CAS 7778-50-9, Fisher). High voltage direct current power supply was provided by a system from Gamma High Voltage Research Inc., Ormond Beach, Florida, model ES30P-5W. A syringe pump was purchased from Cole-Parmer Instrument Company (series 74900). The UV-visible spectrometer used is

Genesys 20 from Thermo Scientific, with a 300w ELS-2 Xenon-arc lamp purchased from Solos Endoscopy Incorporation.

3.2 Preparation of TiO_2/PAN nanofiber

3.2.1 Electrospinning

An electrospinning dope was prepared as follows. 2 g of PAN powder was added into 10 ml of DMSO in a beaker then mixed by a magnetic stirrer until a vicious and transparent polymer stock solution was formed. TIIP was chosen to be the precursor for TiO_2 nanomaterial (Li and Xia 2003, Chandrasekar, Zhang et al. 2009). 2 ml of TIIP and 0.8 ml of acetone were gradually added into the mixture of 6 ml PAN stock solution and vigorously mixed in a small glass vial in 1 hour to provide the electrospunable supporting substrate for the electrospinning process. The whole solution was fully mixed before loaded into a syringe.

The syringe needle diameter is of 22 G, and connected to a high voltage direct current power supply. A roller grounded aluminum foil was used as a collector and placed 5 cm away to the needle tip. A voltage of 15~20kV was supplied between the needle and the collector by a DC generator. Pumping was provided by a syringe pump at the rate of 0.025 ml/min. All of the above preparations were undertaken inside a fume hood at room temperature. The schematic diagram is shown in figure 3.1.

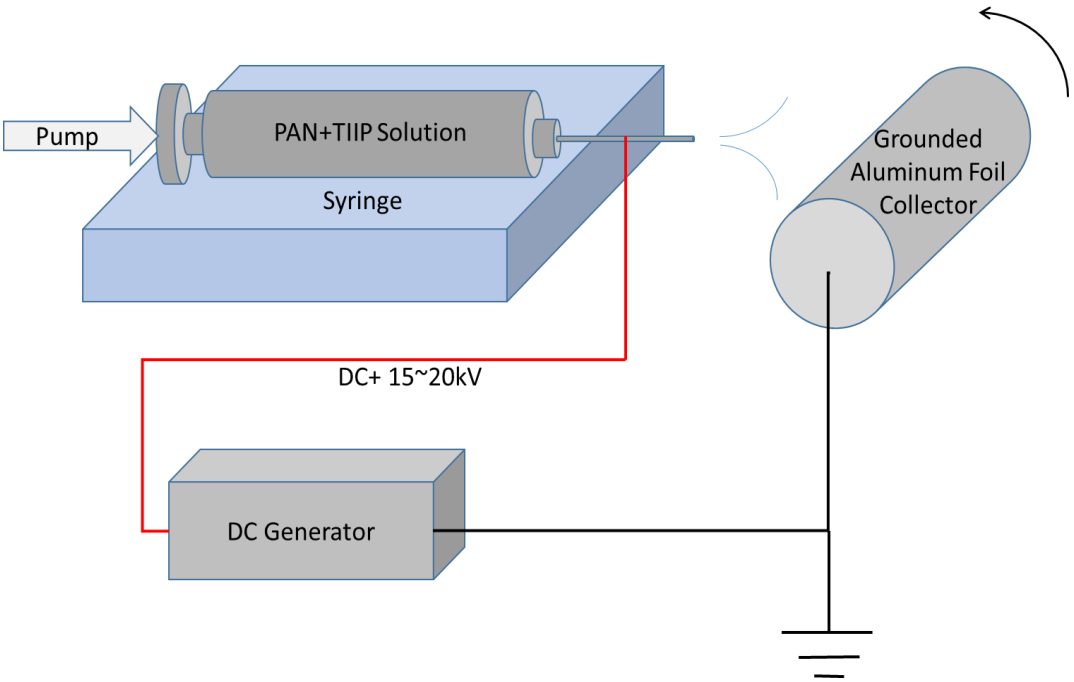

Figure 3.1 Schematic diagram of equipment set up for electrospinning of PAN/TiO2 nanofibers.

3.2.2 Post preparation and annealing

After the electrospinning process, the mixture was electrospun to produce a thin layer containing of polymer fibers coated/filled with TIIP attached on the aluminum foil collector and then the foil was dried in an oven at 105°C for 2 hours. The foil was placed in DI water for 24 hours to allow a complete hydrolysis for TIIP to convert into amorphous TiO_2 following the reaction as below:

$$Ti(OPr)_4 + 4\ H_2O \rightarrow TiO_2 + 4\ Pr\text{-}OH$$

The foil was annealed at 300°C in a muffle furnace for 6 hours with the heating rate of 5°C/min, which changed the amorphous TiO_2 into crystalized forms of anatase and rutile within the nanofiber structure. During this annealing process, carbon and nitrogen in the PAN were doped onto TiO_2 crystal surfaces, and as a result, the TiO_2/PAN nanofibers

could be activated under visible light irradiation (Nguyen and Deng 2012). After the annealing process, the foil with nanofibers mat was slowly cooled down to room temperature and cut into the desirable size prior to storage and use. The tested specimen is the mat of nanofibers collected on the alumina foil with size of 4cm*4cm.

3.3 Determination method of Cr(VI)

There are many methods reported for the determination of Cr(VI) with various sensitivities. Ion chromatography and colorimetry are two most common approaches for quantifying Cr(VI) in the liquid phase. According to EPA METHOD 218.7-Determination of Cr(VI) in Drinking Water by Ion Chromatography with Post Column Derivatization and UV-visible Spectroscopic Detection, the detection limit (DL) of this method could be as low as 0.0044 μg/L, indicating a very trace amount of Cr(VI) that is much lower than the California Public Health Goal level (0.2 μg/L) can be detected. However, this method needs substantial effort for sample preparation so may not be suitable for routine monitoring of chromate as needed in studying its reduction kinetics.

The determination of Cr(VI) in this research is based on the EPA METHOD 7196A-Chromium, Hexavalent (Colometric) and national standard of China-GBT 7467-87. This colorimetry method has sufficient sensitivity and is easy to operate. In the method, the dissolved hexavalent chromium reacts with 1-5-diphenylcarbazide ($C_{13}H_{14}N_4O$) in an acidic solution producing a violet colored compound of unknown composition, and in the absence of interfering amounts of substances such as molybdenum, vanadium, and mercury, the absorbance measured at 540 nm is proportional to Cr(VI) concentration. A pH around 2 was controlled for color development by H_2SO_4 (9.21 mol/L) and H_3PO_4 (7.32

mol/L). 0.04g 1-5-diphenylcarbazide was dissolved in 10mL D.I. water and 10mL acetone as the solvent for the dissolution of 1-5-diphenylcarbazide. Fresh 1-5-diphenylcarbazide solution should be prepared daily before the experiment and discard when the solution becomes discolored. The total volume of the testing sample is 7.50 mL, with 75μL H_2SO_4 solution, 75μL H_3PO_4 solution, 300μL chromogenic agent, and 7.05 mL Cr(VI) solution. A calibration curve of Cr(VI) with concentrations from 0 to 1.00 mg/L was prepared for each reduction experiment, and as shown by Figure 3.2, there was good linear relationship between the absorbance and concentration. In the reduction experiments, 1.50 ml of solution was collected from the reaction system and diluted so Cr(VI) concentration would fall within the range of the calibration curve.

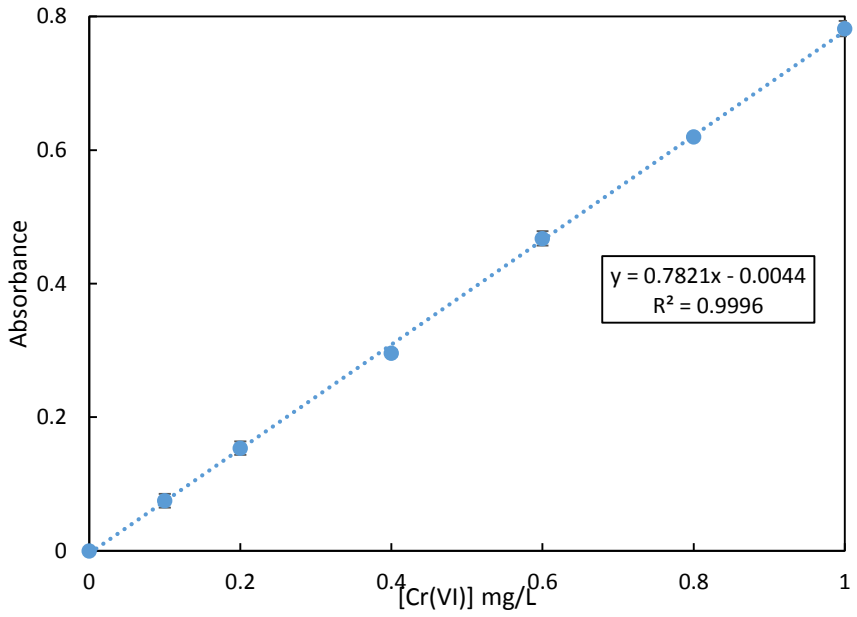

Figure 3.2 Calibration curve Cr(VI) Standard solution

3.4 Removal of Cr(VI) on TiO_2/PAN Nanofibers

3.4.1 Adsorption of Cr(VI) by TiO_2/PAN Nanofibers

The adsorption of Cr(VI) on TiO_2/PAN nanofibers was determined in the dark by measuring spectral changes in 48 hours of a 40 ml of 5mg/L (100µM) Cr(VI) solution at pH of 2.5, 7.0, 8.5 (adjusted by H_3PO_4, NaH_2PO_4,Na_2HPO_4 and NaOH) and a TiO_2/PAN nanofibers mat with a size of 4cm*4cm (approximately 0.200 g). All solutions were prepared with D.I. water. The Cr(VI) concentration in reaction system was adjusted by the Cr(VI) standard solution. At fixed time intervals, 1.5 ml Cr(VI) solution was collected from the beaker and filtered through 0.2 µm nylon membrane filters to remove the solid phase from the dissolved phase. The concentration of Cr(VI) was determined by the UV-vis spectrophotometer using the absorbance at 540nm as described previously. The adsorption experiments were also used as a control to evaluate the effectiveness of TiO_2/PAN nanofibers mat as a photocatlyst for Cr(VI) reduction.

3.4.2 Photorcatalytic reduction of Cr(VI) by TiO_2/PAN Nanofibers

Similar to the adsorption experiments, the Cr(VI) solution with the initial concentration of 5mg/L (100µM) was used to examine the photocatalytic reduction of Cr(VI) by TiO_2/PAN Nanofibers. A 40 mL of Cr(VI) solution was taken into the beaker with a desired pH value (2.5, 5.0, 7.0, 8.5). The pH values of the reaction systems were adjusted by H_3PO_4, NaH_2PO4, Na_2HPO4 and/or NaOHAS as the buffer. A TiO_2/PAN nanofibers mat with a size of 4cm*4cm and weight of 0.2g was place in the beaker and directly faced the light source.

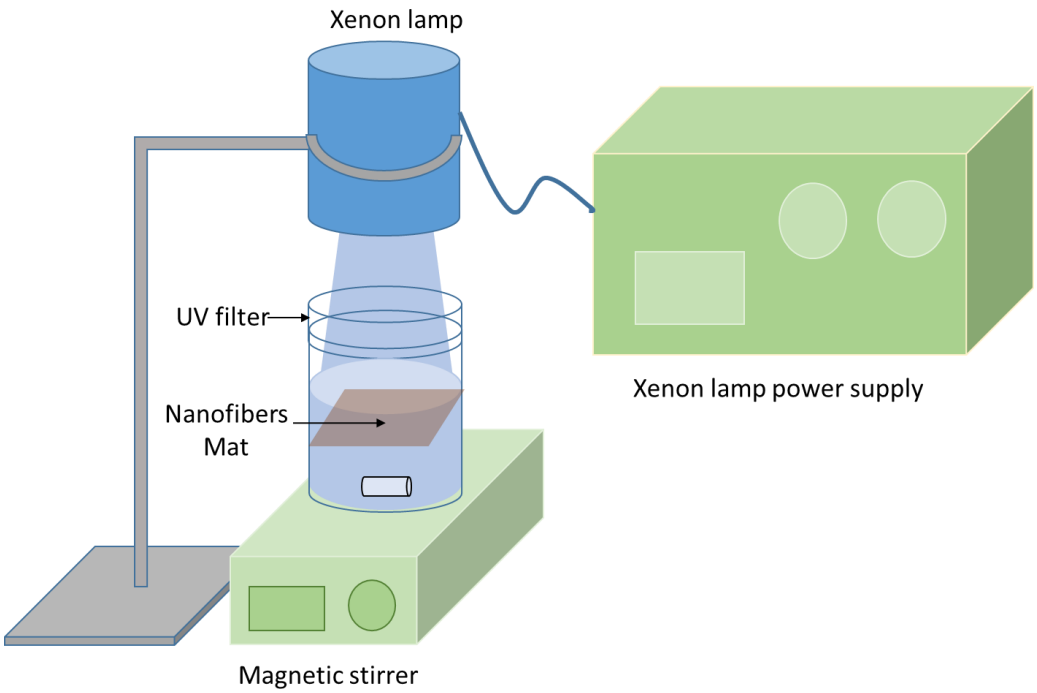

Figure 3.3 Experimental set up used to test photocatalytic reduction of Cr(VI)

A xenon arch lamp (300w) was used as a light source that includes both visible and UV radiations. A UV filter was used to eliminate the UV portion of the wavelengths shorter than 400 nm. To eliminate the effect of solution evaporation, a low-density polyethylene wrap was used to cover the beaker when testing the effect of UV, with an assumption that the UV can have a 100% transmission through the cover. For the visible light source, the size of the UV filter was fitted to the diameter of the beaker which meant that the UV filter has not only blocked the UV light from the xenon arc lamp but also minimized evaporation of the solution. The experiment set up is shown in figure 3.3.

To investigate the effect of the humic acid (HA) on the photoreduction rate, we first prepared the HA stock solution by dissolving a certain amount of the HA solid powder in the D.I. water, with pH adjusted to 8~9 by NaOH. Near complete dissolution of HA powder occurred upon shaking for 24 hrs, then the solution was filtered through 0.45 µm

membrane filter to remove any insoluble residual, and solution pH adjusted to neutral by H_3PO_4 . The total organic carbon(TOC) of the HA stock solution was measured by the Shimadzu TOC-V total organic carbon analyzer coupled with ASI-V autosampler. Different volumes of the HA stock solution were added to make the various HA concentration (TOC) of 2.0, 4.0, 8.0 mg/L in the Cr(VI) reaction system.

At fixed time intervals, 1.5 ml Cr(VI) solution was collected from the beaker and filtered through 0.2 μm membrane filters to separate the solid phase from the dissolved phase. The concentration of Cr(VI) was determined by the UV-vis spectrophotometer.

3.5 Data analysis and modeling

During the degradation of Cr(VI) by photocatalysis, the concentrations of the photocatalyst or DI water remains essentially constant. Many researchers have observed that the Cr(VI) photocatalytic reduction could be described by the pseudo first-order kinetics model:

$$r = -\frac{dC}{dt} = K'C \qquad (3.1)$$

k' is the pseudo first-order rate constant with a unit of time^{-1}; C is the concentrations of aqueous Cr(VI); t is the illuminated (reaction) time and r is the reaction rate.

The equation 3.1 can be changed into the linear form:

$$\ln\left(\frac{Ct}{C0}\right) = -K't \qquad (3.2)$$

Where C_t is the concentration of Cr(VI) at time t, and C_0 is the initial concentration of the Cr(VI).

As indicated above, the original data collected was represented by the absorbance from UV-visible spectrometer. The concentration of Cr(VI) is proportional to the

absorbance. Thus, we can easily get that C_t/C_0 is equal to Ab_t/Ab_0, where Ab_0 and Ab_t are the absorbance of aqueous Cr(VI) when illuminated at time 0 and t, which means:

$$\ln\left(\frac{Ab_t}{Ab_0}\right) = -K't \qquad (3.3)$$

A series of data points can be fitted to a straight line when ln (Ab_t/Ab_0) is plotted against time. The apparent pseudo first-order rate constant k' is represented by the negative value of the slope. For the purpose of calculating the pseudo first-order rate constant, the collected data after the time when the system temperature remained constant and less than 90% of the final removal efficiency were used.

Reference

"Chromium, Hexavalent (Colometric)." U.S. Environmental Protection Agency,Method 218.6; Cincinnati, OH (1992).

"Determination of Cr(VI) in Drinking Water by Ion Chromatography with Post Column Derivatization and UV-visible Spectroscopic Detection." U.S. Environmental Protection Agency,Method 218.6; Cincinnati, OH (2011).

"Determination of Dissolved Hexavalent Chromium in Drinking Water, Groundwater, and Industrial Wastewater Effluents by Ion Chromatography." U.S. Environmental Protection Agency,Method 218.6; Cincinnati, OH (1991).

Chandrasekar, R., et al. (2009). "Fabrication and characterization of electrospun titania nanofibers." Journal of Materials Science **44**(5): 1198-1205.

EPA (2011). "EPA's recommendations for enhanced monitoring for Hexavalent Chromium (Chromium-6) in Drinking Water." **Retrieved**

Li, D. and Y. Xia (2003). "Fabrication of titania nanofibers by electrospinning." Nano Letters **3**(4): 555-560.

Nguyen, H. Q. and B. Deng (2012). "Electrospinning and in situ nitrogen doping of TiO2/PAN nanofibers with photocatalytic activation in visible lights." Materials Letters **82**(0): 102-104

Chapter 4 EXPERIMENTAL RESULTS AND DISCUSSION

4.1 Characterization of TiO_2/PAN nanofibers

The as-prepared TiO_2/PAN nanofibers were characterized by SEM and BET analysis. As shown in Fig. 4.1.1, TiO_2/PAN retained the fibrous shape, with fiber diameters ranged from around 400 nm to greater than 1 μm. The EDS analysis showed the existence of element C, O, N, and Ti in the annealed TiO_2/PAN nanofibers. In Nguyen and Deng's research report, more characterization experiments were conducted. EDS pattern of the annealed fibers showed that a portion of H-titanates which was formed by the hydrolyzed amorphous TiO_2 at around 300^{o}C during the annealing process has been converted into anatase in the annealed nanofibers. The UV-VIS spectra also verified that the peak absorption band shifted to 370-390 nm, proving that H-titania has been converted at least partially into anatase during the annealing process. (Nguyen and Deng 2012). The initial SEM image of TiO2/PAN nanofiber made by Nguyen and Deng is shown in figure 4.1.1 (a)

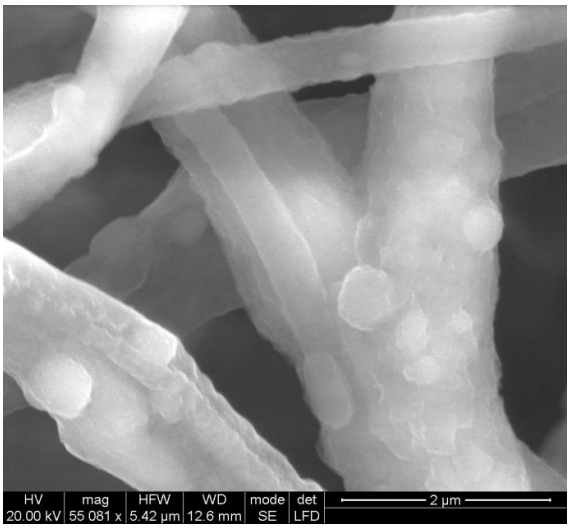

(a)

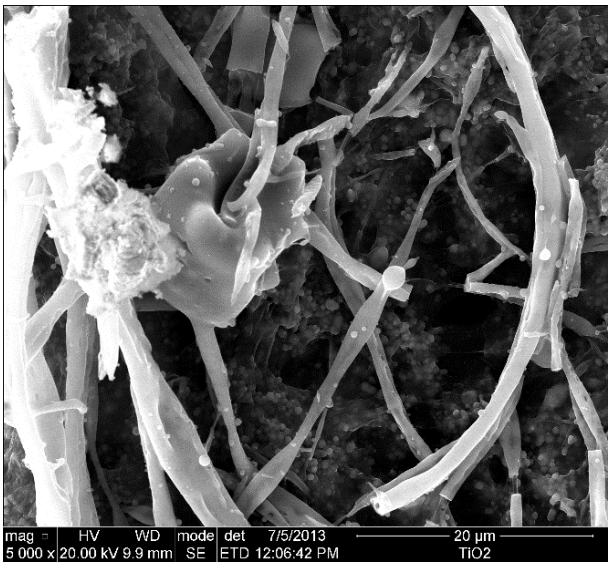

(b)

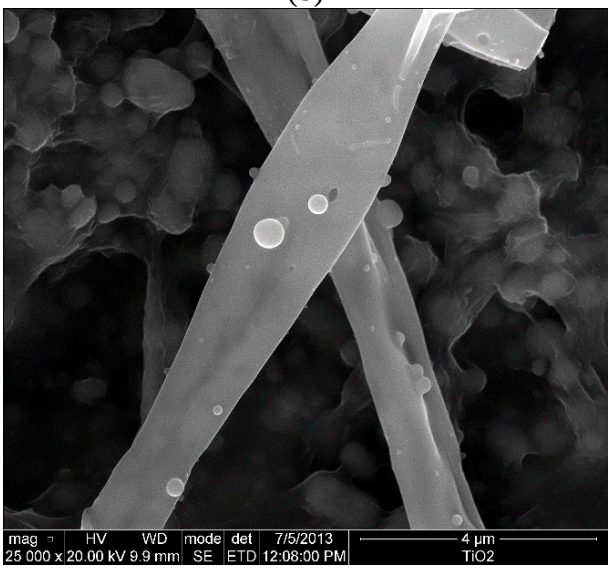

(C)

Figure 4.1.1 SEM images of the TiO2/PAN nanofibers

Fig 4.1.1 (b) and (C) are the SEM images of annealed TiO_2/PAN nanofibers fabricated in our research, showing that annealedThe BET test showed that the specific surface area (SSA) of PAN/TiO_2 nanofibers mat was 24.759 m^2/g. It seemed that the SSA value of the TiO_2/PAN was much lower than the other TiO_2 nanomaterials. This could be explained by the modified synthesis process of the nanofibers. In the previous research (Li and Xia

2003), the annealing temperature for nanofibers was 500 ^{o}C which meant that the polymer solution was evaporated and left only the pure porous TiO_2 nanofibers after the annealing process. However, although the pure porous TiO_2 has a great SSA, it was not suitable for proposed application because of its poor mechanical strength. In order to enhance the physical properties of the TiO_2 nanofibers, the annealing temperature was decreased to 300 ^{o}C to keep the polymer substrate such as PAN in the nanofibers according to the preparation method created by Nguyen and Deng (2012).

During the synthesis of TiO_2/PAN nanofibers, the major problem was to keep the electrospinning process smooth which meant that the needle would not be blocked by the electrospinning solution. In the preliminary experiment for synthesizing the nanofibers, electrospun mixture showed the tendency of blocking the flow rapidly within 10-15 minutes under the room temperature. The blocking could be controlled by adding acetone in the solution. The acetone was added to improve the fluidity and the evaporation rate of the electrospun mixture. However, the excess addition of acetone decreased the viscosity of the electrospinning solution, resulting in many beads formed among fibers and blocking the needle during the electrospinning process. It was found that an addition of 0.6ml of acetone could ensure a smooth electrospinning process. With this volume, the nanofibers form the fibrous shape on the collector because of the appropriate evaporation rate. It appeared that other one of the main factors of blocked-needle problem was caused by PAN. Eventually we mounted a heating lamp to increase the temperature of the electrospinning process. 0.8ml of acetone was added in the following synthesis process to ensure the formation of nanofibers on the controller.

According to a previous report (Nguyen and Deng 2012), the nanofibers foil sheet after electrospinning should be folded two or three times, so the nanofibers could be removed from the foil and cut into the piece with size of 1.5cm*1.5cm. The purpose was to improve the mechanical strength and density of the nanofibers. However, the optical thickness of the nanofibers (15μm) (Shaham Waldmann and Paz 2010) is much smaller than the thickness of the pieces. In addition, the size of the pieces was comparably difficult to control because the nanofibers would shrink or twisted during the following annealing process. The surface area and 3-dimensional shape of the nanofiber pieces was not easy to maintain. In contrast, the nanofibers mat attached on the foil without folding did not have the same problems as the pieces. Nguyen and Deng's research indicated that the TiO_2/PAN thin pieces can be rinsed with the water jet from laboratory D.I. water bottle and transferred among containers by tweezers without being broken. However, the photocatalytic degradation of Cr(VI) experiments in neutral or basic condition under the visible light would take a very long time (up to 3 days), the mechanical strength of the TiO_2/PAN nanofibers piece could not endure such long time irradiation in the liquid phase and be easily broken or dissolved in the Cr(VI) solution. The nanofibers mat attached on the foil should perform better in the practical application of Cr(VI) photoreduction for its better mechanical strength.

4.2 Adsorption of Cr(VI) on TiO_2/PAN Nanofibers

Figure 4.2.1 presents the adsorption kinetics of Cr(VI) on the PAN/TiO_2 nanofibers at four different pH conditions: pH=2.5, 5, 7, 8.5. All tests were performed at room temperature (20 ± 2 ^oC) with the same surface area, weight of mats, and Cr(VI) initial concentration in the dark. The data showed that there was only a small amount of Cr(VI) (less than 5%) adsorbed on the TiO_2/PAN nanofibers in the dark within 48 hours under all pH conditions. This result was consistent with the reports in the literature that the adsorption has little effect on the removal of Cr(VI) by TiO_2 (Ku and Jung 2001, Shaham Waldmann and Paz 2010). The loss of Cr(VI) could not only be resulted from the TiO_2/PAN nanofibers, but also by the sorption on the glass wall of the beaker. It seemed that the optimal pH value for the adsorption of Cr(VI) by TiO_2/PAN nanofibers was around 5.0. This might be explained by the changes of Cr(VI) speciation and solid surface functional groups with pH in the aqueous solution. The concentrations of negatively-charged Cr(VI) species such as $HCrO_4^-$ and CrO_4^{2-} are dominant at pH values greater than 2. The TiO_2 surface carries more positive charges in acidic solution and more neutral or negatively-charged at pH higher than 6 (Ku and Jung 2001). The pH-dependent electrostatic force between the Cr(VI) species and TiO_2 surface could be the main factor resulting in the observed adsorption behaviors. Since the sorbed amounts of Cr(VI) become stables after a few hours, further removal of Cr(VI) concentrations in the photocatalytic experiments under the light irradiation was considered due to the reduction, not sorption.

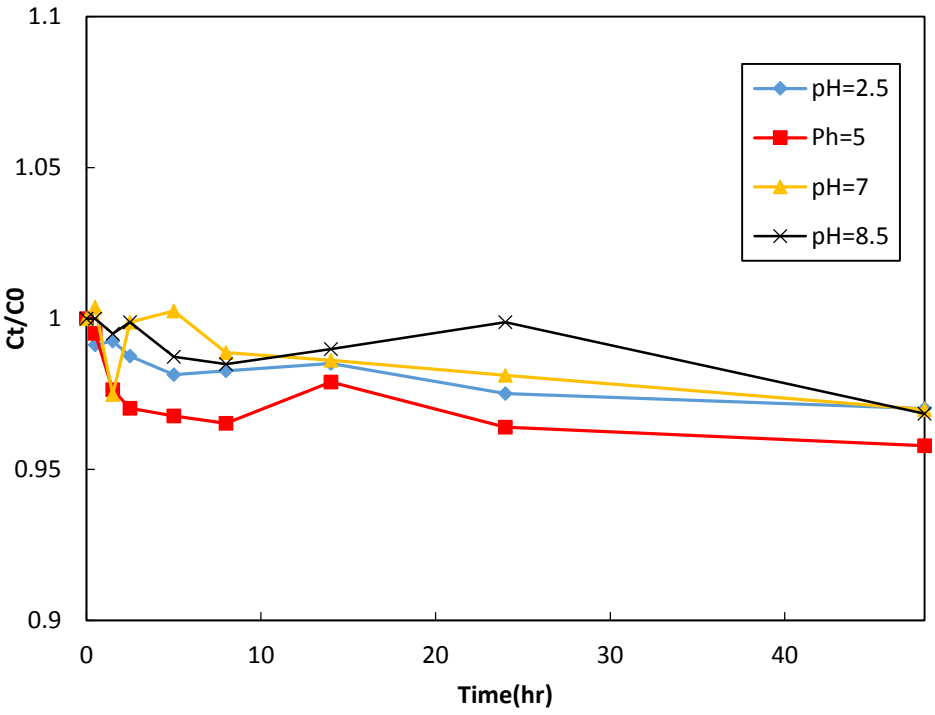

Figure 4.2.1 Kinetic of adsorption of Cr(VI) on TiO_2/PAN nanofobers at different pHs.

4.3 Photoreduction of Cr(VI) by TiO_2/PAN Nanofibers

Before the photoreduction measurement, the variation of the reaction system temperature should be determined at first. Because of the light irradiation, the temperature of the reaction solution would increase to some degree and reach to a constant value. The measurement result is showed below (Figure 4.3.1).

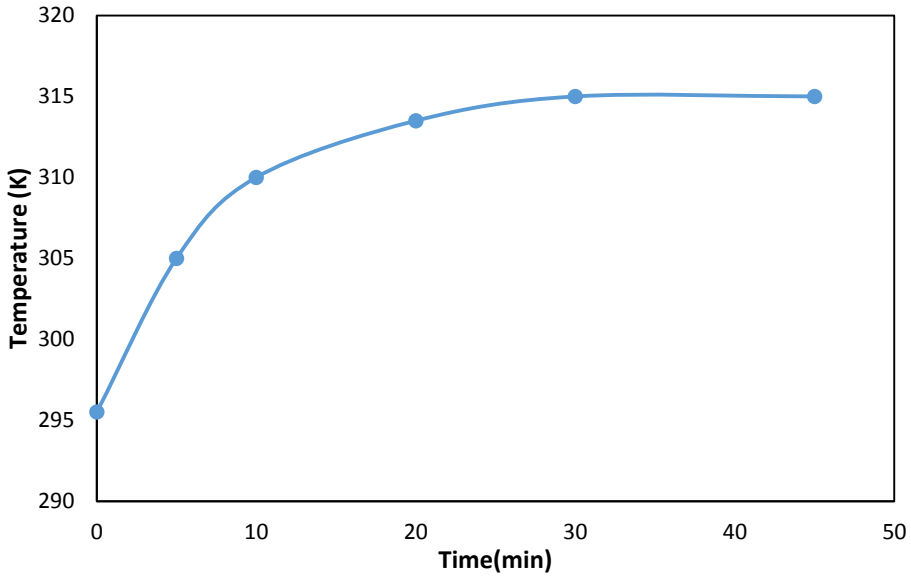

Figure 4.3.1 Variation of reaction system temperature.

The above figure indicated that the reaction system temperature increased from 295.5K (22.5 ^{o}C) to 315K (42 ^{o}C) and unchanged after 30 min. Thus, 315K were consider as the photocatalytic reaction temperature and the reaction rate constant K kept unchanging after 30 min.

The kinetic experiments were conducted by using a 300w xenon arc lamp as the light source to provide both visible light and UV light. To evaluate the effect of TiO_2/PAN nanofibers on the photocatalytic reduction of Cr(VI), a blank test was included that contained no nanofibers but otherwise the same amount of Cr(VI) (5.0 mg/L) and irradiated under the same conditions. The result showed that the homogeneous photochemical reduction of Cr(VI) after 2 days of irradiation was negligible at a neutral pH condition, which is consistent with what was reported in the literature (Khalil, Mourad et al. 1998).

4.3.1 Influence of pH

The concentration changes of Cr(VI) due to its photocatalytic reduction at various pH conditions are shown in Figure 4.3.2. It is clear that Cr(VI) photocatalytic reduction rate increased with decreasing pH values, which is consistent with previous reports (Kabra, Chaudhary et al. 2004). At pH 2.5, almost 100% of the Cr(VI) was reduced after 3 hours; while at pH of 5.0, 7.0, and 8.5, the percentage reduction after 400 min irradiation were 100%, 60%, and 30%, respectively.

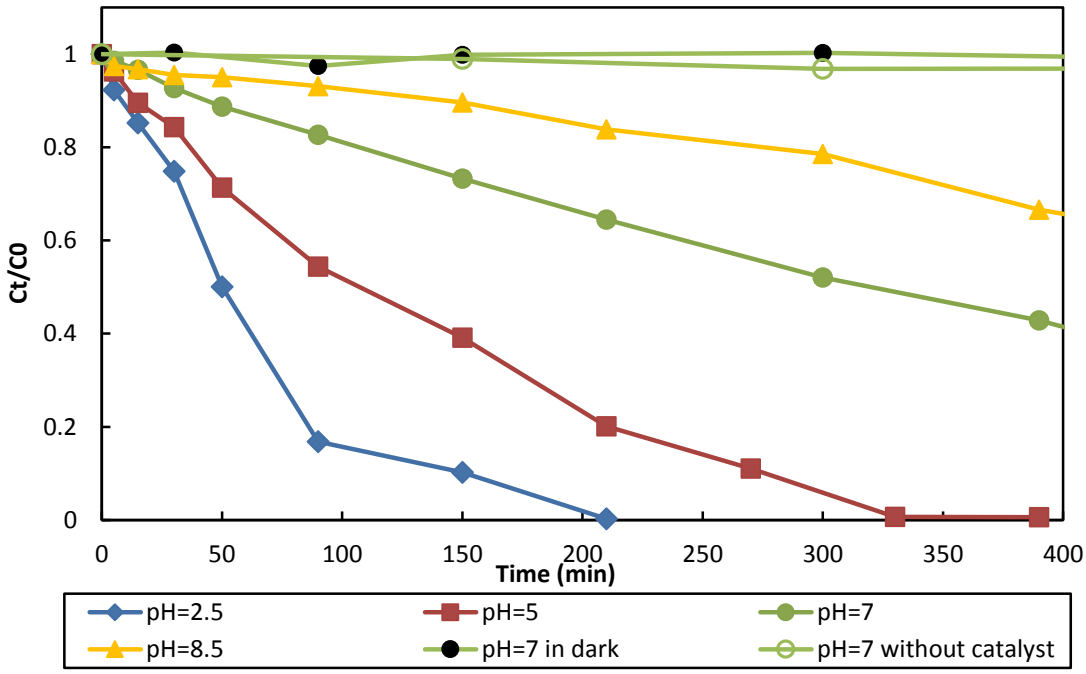

Figure 4.3.2 The Cr(VI) reduction measurements with the initial concentration of 5mg/L(100μM) at different pH conditions under the UV+Visible light within 400min exposure.

Figure 4.3.3 presents the Cr(VI) reduction results at pH 7.0 and 8.5 at a longer duration. The reaction reached certain equilibrium levels after this relatively long irradiation, for example, approximately 1.0 mg/L at pH 8.5. This indicates that not only is the reaction rate strongly affected by the pH but also the degree of reduction.

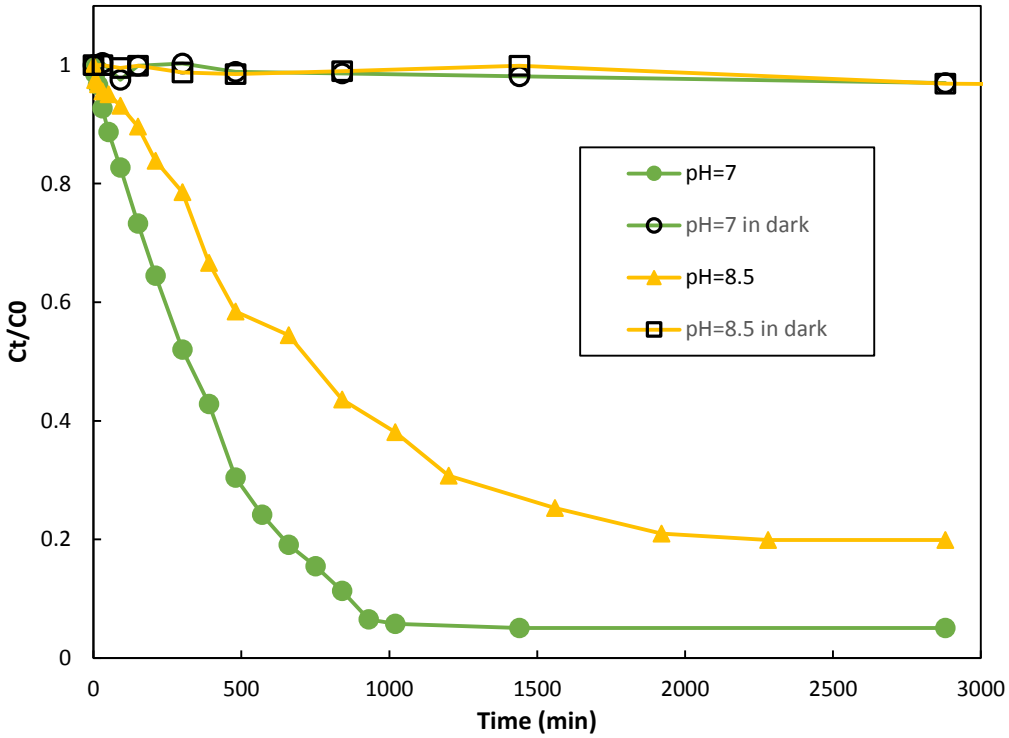

Figure 4.3.3 The Cr(VI) reduction measurements with the initial concentration of 5mg/L(100μM) at pH of 7and 8.5 under the UV+Visible light within 2 day (2880 min) exposure.

The kinetics of Cr(VI) photoreduction under different pH conditions were analyzed by the pseudo-first order kinetic model. As shown by Figure 4.3.4, the $\ln(C_t/C_0)$ versus time plots are linear, from which the pseudo first order rate constants can be obtained. The data (C_t/C_0) after 30 min (when the system temperature remained constant as mentioned in the previous part) and before reach 90% of the final removal efficiency were picked up to make the kinetics plots. The calculated results of rate constant, coefficient of determination (R^2) and the efficiency of removal are listed in Table 4.3.1.

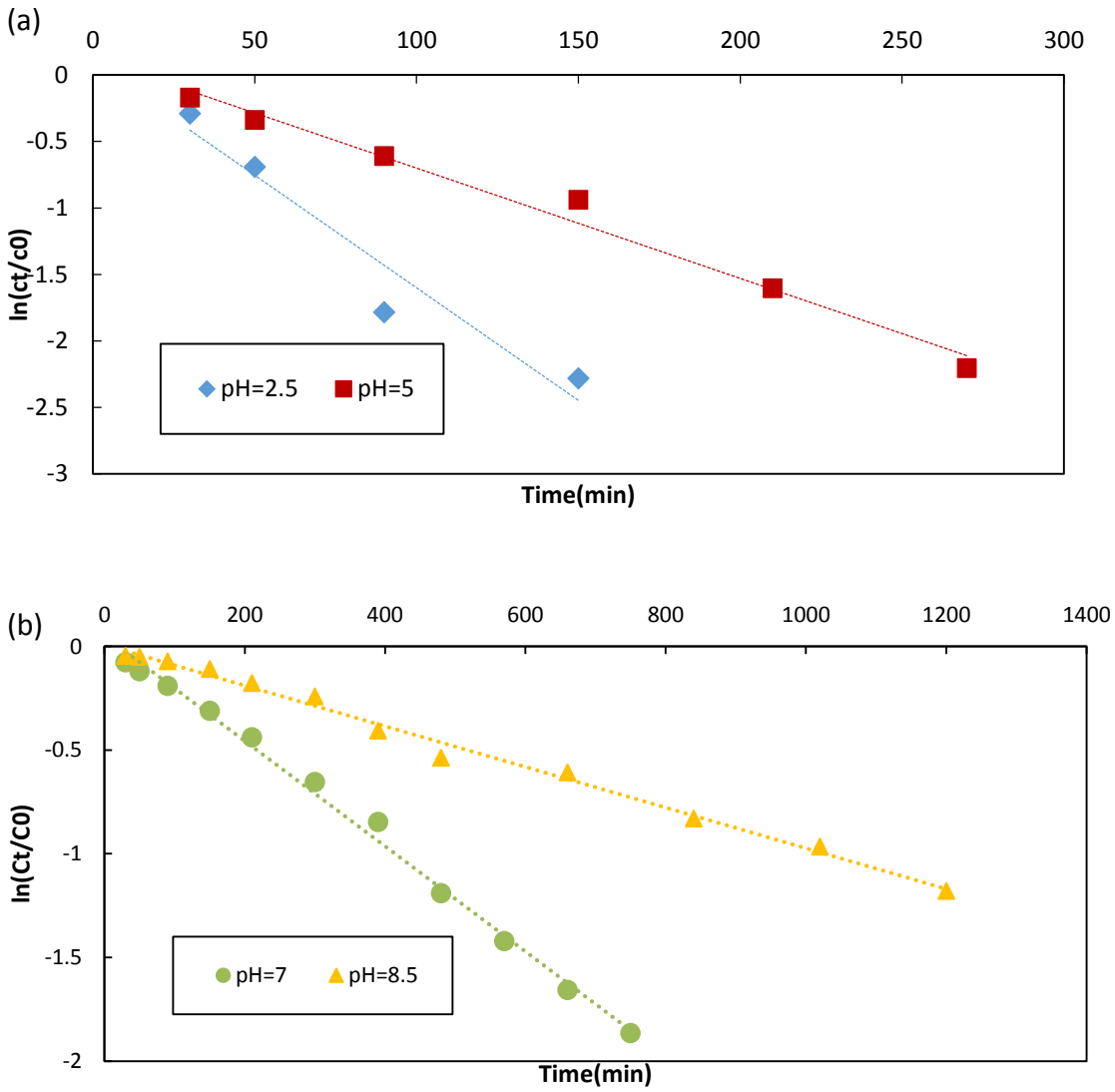

Figure 4.3.4 The pseudo-first order kinetics plots for Cr(VI) catalytic reduction at pH of 2.5, 5 (a) 7, 8.5 (b) under UV+visible light.

Table 4.3.1 Rate constants at various pHs

pH	light resorce	K(min^{-1})	R^2	Removal Efficiency
2.5	UV+Visible light	0.0169	0.933	→100%
5	UV+Visible light	0.0083	0.985	99.40%
7	UV+Visible light	0.0025	0.995	94.97%
8.5	UV+Visible light	0.0010	0.992	80.12%

The results indicated that Cr(VI) reduction rates were higher at acidic pH than at neutral or basic pH conditions. This pH dependence might be due to the higher reduction potential of Cr(VI)/Cr(III) half reaction at lower pH, so as pH decreases, the thermodynamic driving force for Cr(VI) reduction increases (Lin, Wei et al. 1993, Cappelletti, Bianchi et al. 2008). At a basic condition, the driving force for the reduction of molecular oxygen is higher than for the Cr(VI) and as a result, O_2 may compete for the photo-generated electrons and decrease the rate of Cr(VI) reduction. Moreover, The pH at zero point charge (pHzpc) of P-25 TiO_2 is around 7 (Ku and Jung 2001). It is reasonable to assume that anionic species of Cr(VI) such as CrO_4^{2-} and $HCrO_4^-$ can be easily adsorbed onto the TiO_2 surface used in this study below the pH_{zpc}, thus accelerates the rate of reaction.

Since the mat of TiO_2/PAN nanofibers has the advantage of easy separation and recovering from the reaction solution, the activity of the recovered nanofibers were also tested. The used nanifibers mat was washed gently by D.I. water for several times, soaked in the D.I. water for 2 hours and dried in the oven. The test result is showed in Figure 4.3.5.

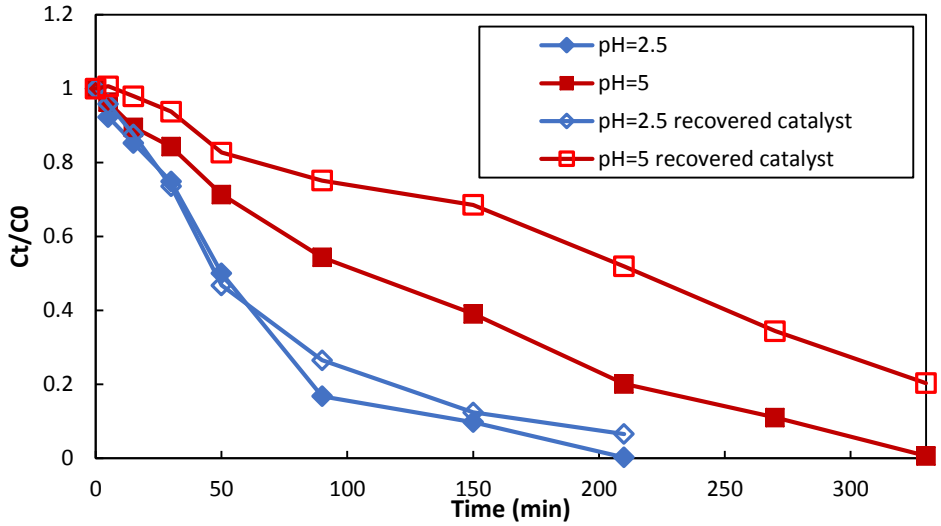

Figure 4.3.5 The recovered TiO_2/PAN nanofibers performance of Cr(VI) photocatalysitc reduction.

It is clear that the recovered nanofibers from the reaction solution at pH 2.5 showed almost the same photocatalytic ability as the virgin nanofibers. However, the photocatalytic performance of the recovered nanofibers from the test at pH 5.0 declined significantly in comparison with the original nanofibers. At pH 7.0, the reaction took much longer (> 16 hrs) to complete, and it was observed that the color of the nanofibers changed from dark brown to gray white under this long irradiation. The recovered nanofibers at pH 7 showed very poor photocatalytic activity. The reason for answering the decreased performance of recovered nanofibers was not completely clear. However, a similar observation has been reported in the literature (Kabra, Chaudhary et al. 2004).

There were reports that Cr(III) formed a stable precipitate on the catalyst and fouled the photocatalyst at pH higher than 4 (Prairie, Evans et al. 1993, Giménez, Aguado et al. 1996). Supporting view by other research also indicated that fouling of the photocatalyst happened at pH above 4 (Giménez, Aguado et al. 1996). In a study by Ku and Jung, the used TiO_2 particles after photocatalytic Cr(VI) reduction was analyzed by ESCA. Cr on

the surface of TiO_2 particles was identified to be Cr(III), while no indication of the presence of Cr(VI) (Ku and Jung 2001), suggesting potential fouling by the precipitated Cr(III).

The BET test for measuring the specific surface area may also prove the fouling of the nanofibers to some degree. The SSA of the recovered nanofibers at pH 7.0 decreased from 24.8 m^2/g to 14.1 m^2/g. The EDS spectra confirmed that there was Cr element on the surface of the recovered nanofibers. However, the presence of Cr element could be partially due to sorption of Cr species instead of precipitation. In addition to the precipitation of Cr(III), the other explanations for the declining performance of the recovered catalyst may include the followings. The TiO_2/PAN nanofibers dissolved in the solution after several hours' illumination to some extent; The surface structure of the nanofibers was destroyed for its inherent brittleness as the pure TiO_2 fibers (Kim, Cho et al. 2010) and loss of mechanical stability during the long time reaction. For the purpose of figuring out the structure of the recovered nanofibers from the solution at higher pH, SEM test was done again. The SEM image is showed in figure 4.3.6. The result suggests that the fiber was modified to certain degree.

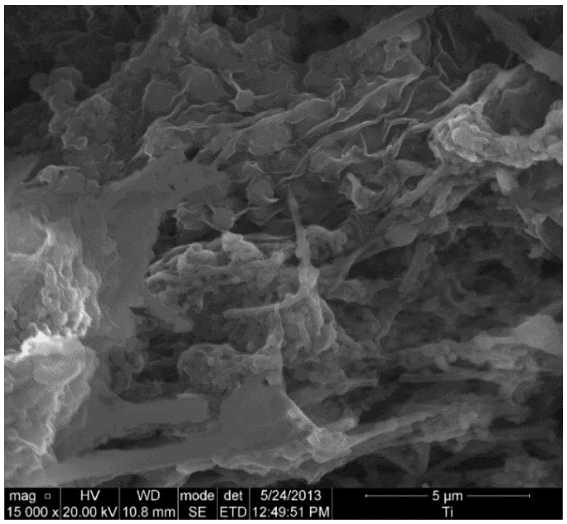

Figure 4.3.6 SEM images of the recovered TiO_2/PAN nanofibers at pH of 7.

As pointed out in Kim and Chao's research, although the synthesis of the TiO_2 nanofibers has been improved with the substrate of PAN and lower annealing temperature (300 ^oC), part of the nanofibers still broke into rod or aggregated after reaction which has restricted its practical application to some degree.

4.3.2 Influence of light source

Based on Nguyen and Deng (2012), nitrogen or carbon provided by PAN was doped into the TiO_2/PAN nanofibers during the annealing process, resulting in a material that could be activated with visible light. One goal of this study was to assess if the visible light could be used as the sole source for the photocatalytic Cr(VI) reduction in the presence of the as-prepared TiO_2/PAN nanofibers. A Hoya 52mm UV multi-coated filter was equipped on the reaction system to filter out the light with wavelength shorter than 400nm but allow the visible light to pass through. Otherwise, this set of experiments was conducted under the same condition as the pervious tests with different pHs.

As illustrated in Figures 4.3.7 and 4.3.8, light is needed for the reaction to take place as there was no Cr(VI) reduction in the dark controls. When comparing the visible light and UV+visible light, the decrease in Cr(VI) concentration at 150 min under visible light was only about half of the value under the UV+visible light at pH 2.5 and 5.0. At neutral pH condition, the reaction is much slower and only 50% of the Cr(VI) in the solution was reduced after 24 hrs (1440 min). Although the light source has strong effect on the reaction rate, the removal efficiency maintained at the same level at acid and neutral condition under either light source as shown in the figures (Figures 4.3.7 and 4.3.8).

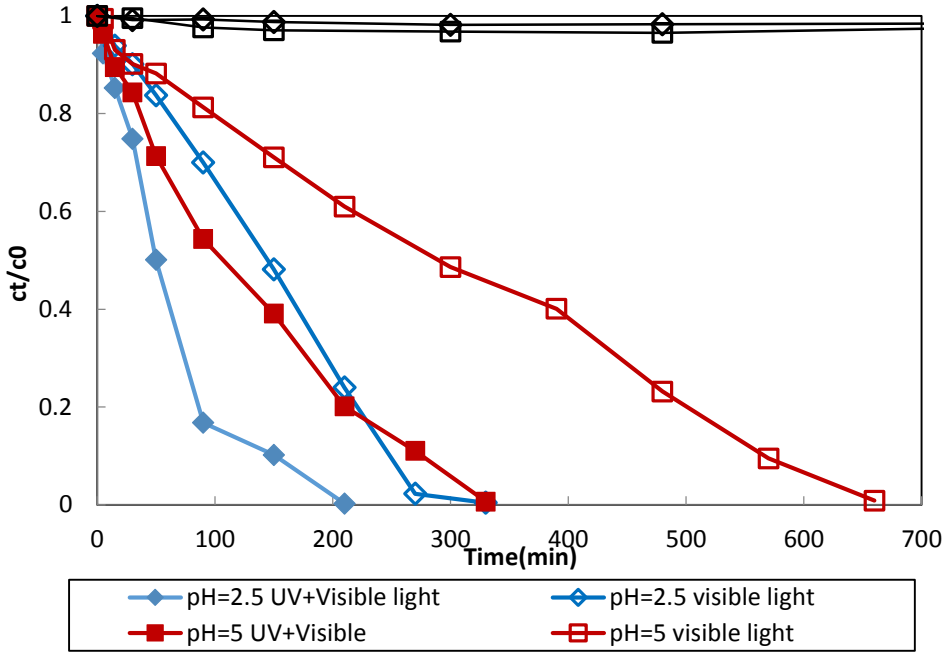

Figure 4.3.7 The Cr(VI) reduction measurements with the initial concentration of 5mg/L(100μM) at pH of 2.5 and 5 under the different light source.

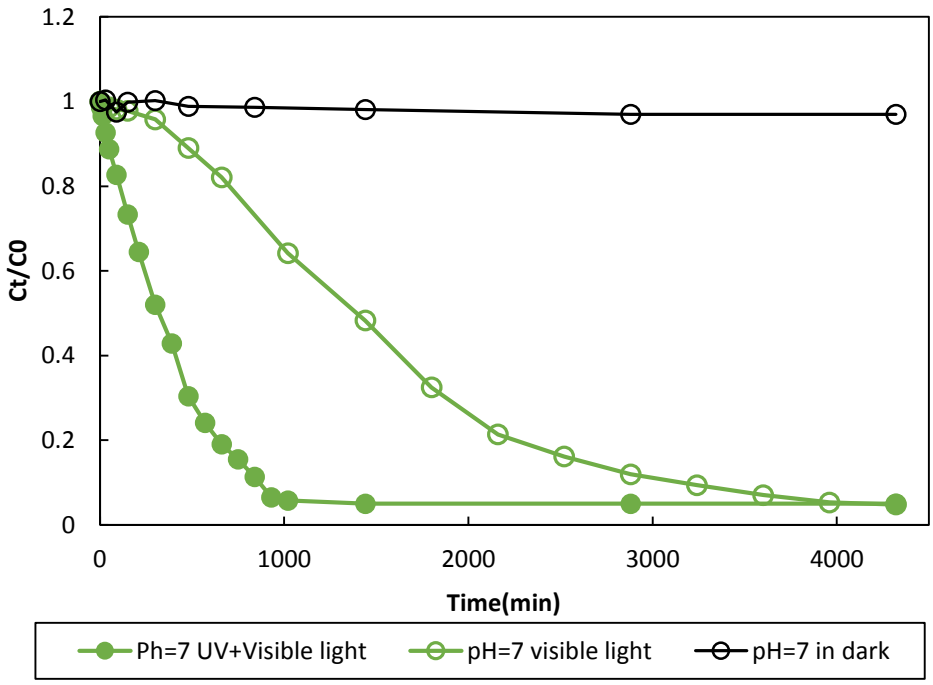

Figure 4.3.8 The Cr(VI) reduction measurements with the initial concentration of 5mg/L at pH of 7 under different light source.

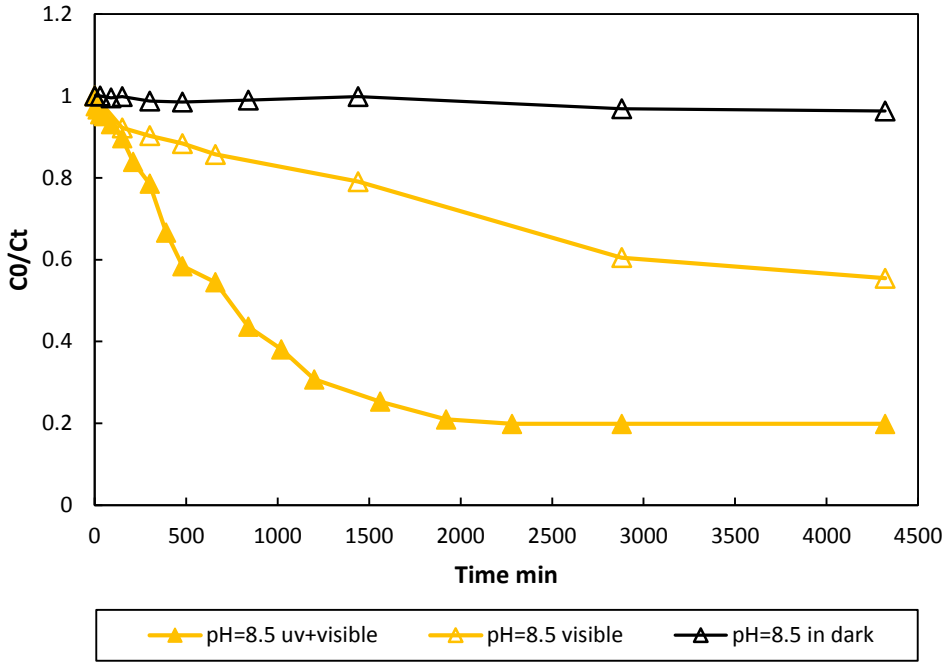

Figure 4.3.9 The Cr(VI) reduction measurements with the initial concentration of 5mg/L at pH of 8.5 under different light source.

However, the situation was not the same for basic solution, as represented in figure 4.3.9. Under the visible light exposure at pH 8.5, not only the reaction rate decreased sharply but also the removal efficiency. Merely 44% of Cr(VI) was reduced after 3 days of visible light irradiation. The pseudo-first order kinetics plots are shown in figure 4.3.10 (a) and (b). The summary and comparison of the calculated reaction kinetic parameters is listed in Table 4.3.2.

Table 4.3.2 kinetic parameters summary

	visible light			UV+Visible light		
pH	K(min^{-1})	R^2	Removal Efficiency	K(min^{-1})	R^2	Removal Efficiency
2.5	0.0072	0.956	→100%	0.0169	0.933	→100%
5	0.0028	0.962	99.16%	0.0083	0.985	99.40%
7	0.0008	0.976	95.18%	0.0025	0.995	94.97%
8.5	0.0002	0.988	44.25%	0.0010	0.992	80.12%

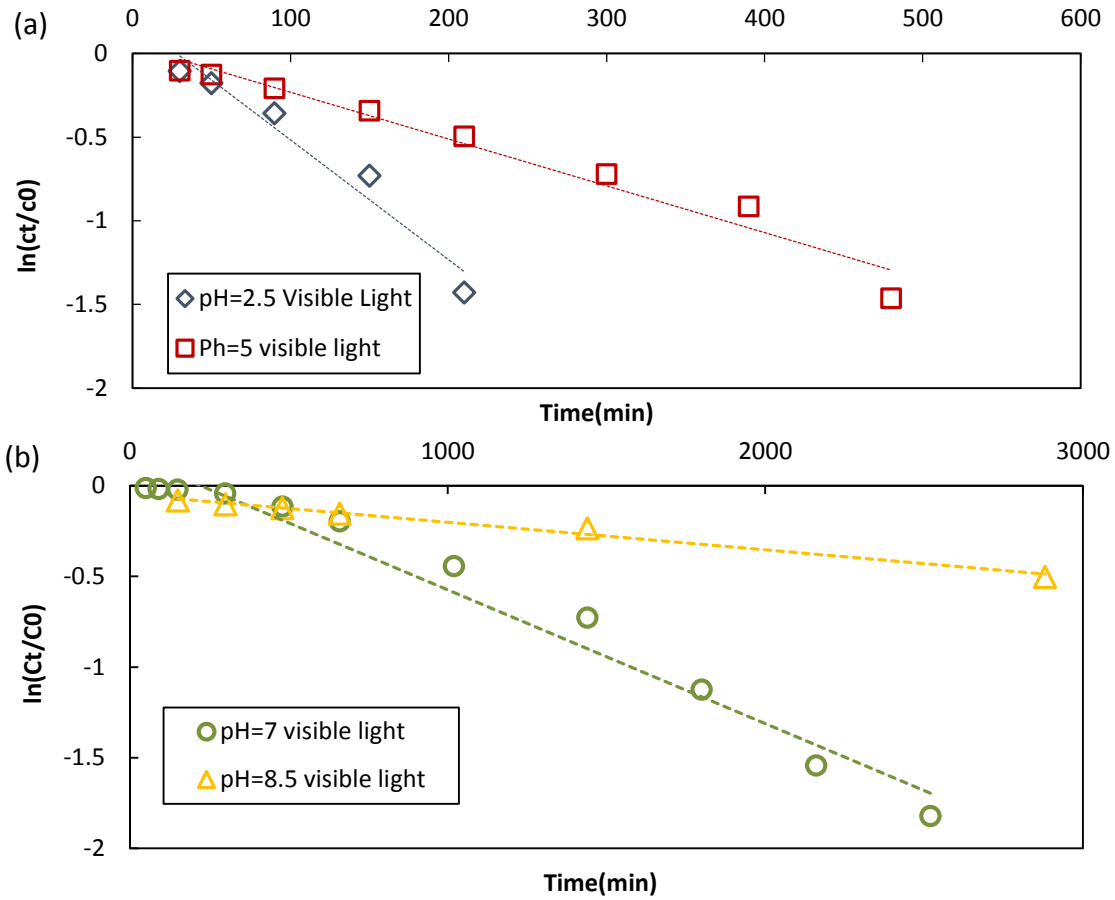

Figure 4.3.10 The pseudo-first order kinetics plots for Cr(VI) catalytic reduction at pH of 2.5, 5 (a) 7, 8.5 (b) under visible light.

The significant decreasing of the reaction rate constant can be directly observed in the table above. The decreasing reaction rate may not only be caused by the light wavelength but also by the fact that the UV filter has blocked part of the light in visible range. Although the wave length of the light has much influence on the reaction rate, the experiment result still confirmed the effectiveness of the TiO_2/PAN nanofibers on Cr(VI) photocatalytic degradation under visible light illumination. The reduction efficiency of the reaction at the acid condition was still kept at a high level. As mention before, the mechanical strength of the recovered nanofibers which had been through long time reaction was not as good as the unused one let alone the photocatalytic performance. However, it still can be concluded that the TiO_2/PAN nanofibers mats have good stability and durability. The structure and

conformation of the nanofibers remained essentially unchanged. Barely a trace amount of the nanofibers peeled off from the substrate foil even after 3 days of reaction. In addition, it is noteworthy that the TiO_2/PAN nanofibers in air are found to be constant over long time. The exposure to the air condition even during 3 months does not cause changes in catalytic activity.

4.3.3 The impact of humic acid (HA)

Natural organic materials exist widely in natural water, so we examined how the natural organic matters could affect the photocatalytic Cr(VI) reduction, using Sigma-Aldrich humic acid as the source. Many organic acids and alcohols could act as the scavengers to eliminate or prevent the recombination of electrons and holes (Yang and Lee 2006). When natural organic materials are added to the photoreduction system, they may scavenge the holes or capture electrons to form species capable of direct Cr(VI) reduction, thus Cr(VI) reduction can be promoted. Heterogeneous photocatalytic possess is known to reduce metal ions with simultaneous oxidation of organic substances (D. C. Cid, D. C. Grande et al. 2012). The reactions between the positive holes and organics are as follows:

$$h\nu + TiO_2 \rightarrow h^+ + e^- \qquad (4.1)$$

$$H_2O + h^+ \rightarrow \cdot OH + H^+ \qquad (4.2)$$

$$\bullet OH + \text{Organics} \rightarrow \cdots \rightarrow CO_2 + H_2O \qquad (4.3)$$

$$h^+ + \text{Organics} \rightarrow \cdots \rightarrow CO_2 + H_2O \qquad (4.4)$$

This set of experiments was carried out under the HA initial concentration (TOC) of 2.0, 4.0 and 8.0 mg/L at neutral and acid pH (pH=2.5) conditions. The tests at neutral condition were further conducted under both visible light and simulated solar light (UV+visible light from Xenon arc lamp) illumination.

Prior to the assessment of the photocatalytic activity of TiO_2/PAN nanofibers in the presence of HA, we examined the removal of Cr(VI) in the system with HA and nanofibers in the dark. The results (Figure 4.3.11) indicated that with an initial Cr(VI) concentration of 5mg/L and 2.0 mg/L of HA at neutral pH, there was approximately 5% decrease in Cr(VI) concentration within 24 hrs. We also investigated the direct Cr(VI) reduction by HA under the UV+visible light exposure, and found there was an 8% of Cr(VI) removal without the catalyst in the tested time period.

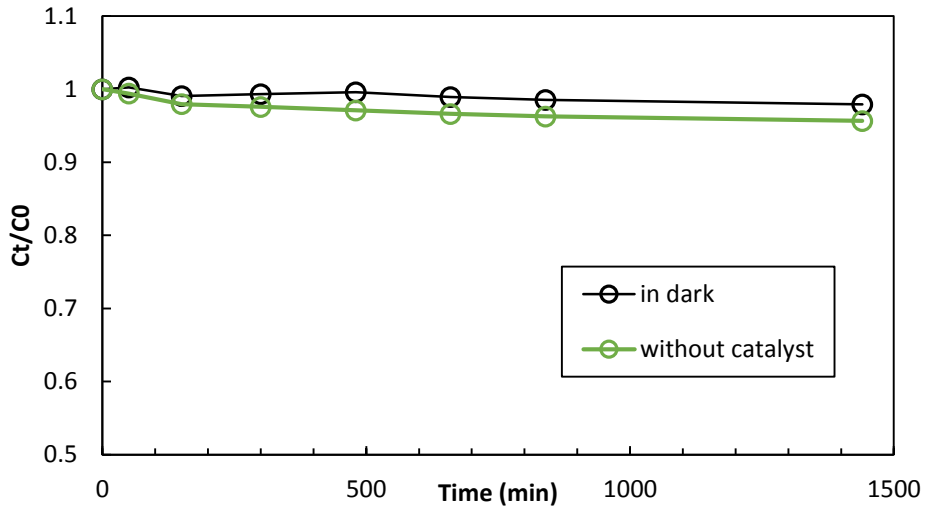

Figure 4.3.11 Control test for Cr(VI) reduction in presence of HA in dark with catalyst and under UV+visible light without catalyst, pH=7, [HA] =2 mg/L.

The changes of Cr(VI) concentration with time under different initial HA concentrations were examined at pH 2.5 (Figure 4.3.12a) and pH 7.0 (Figure 4.3.12b). Under both neutral

and acidic pH conditions, the Cr(VI) concentration had a slightly more decrease in the presence of HA, but the effect was less pronounced at a longer time. While the presence of HA had an effect, increasing HA concentrations from 2.0 mg/L to 8.0 mg/L did not change Cr(VI) concentration profiles. Furthermore, the removal efficiency of Cr(VI) almost kept constant in the systems with or without HA. The concentration of Cr(VI) dropped to below the detection limit at pH 2.5 after 150 min. The situation was similar at near a neutral pH condition, at which the removal efficiency was around 95% .

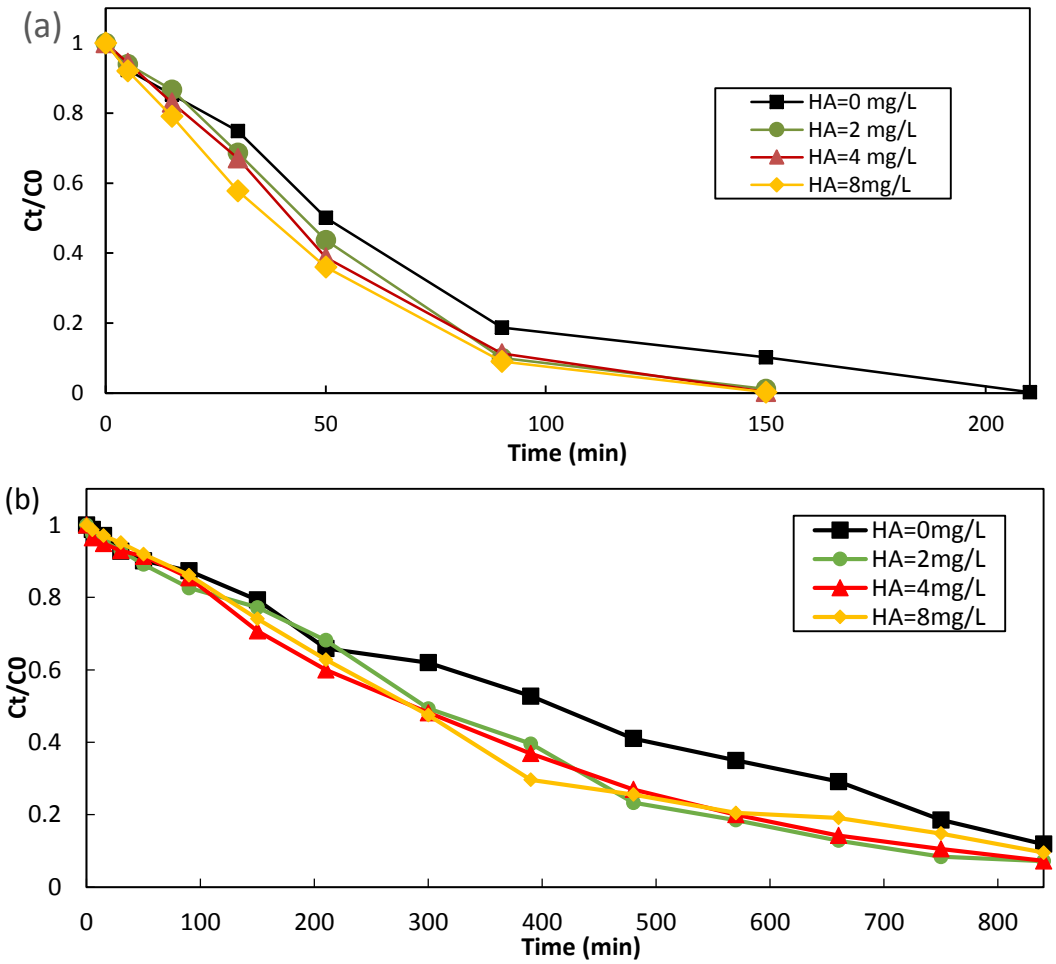

Figure 4.3.12 Effect of HA on Cr(VI) removal under UV+visible light (a) pH=2.5 (b) pH=7

We similarly examined the influence of the HA on Cr(VI) photocatalytic reduction by calculating the pseudo-first order rate constants (Figure 4.3.13 and Table 4.3.3). The results

demonstrated a small but clear increase of the rate constants due to the presence of HA (TOC = 4 mg/L) at both pH conditions. It appeared that HA acted as sensitizers in the photocatalytic reduction of Cr(VI) to Cr(III). One effect of HA is its potential to reduce Cr(VI) adsorption due to its competition for the surface sites. Yet, research has indicated that the oxidation of HA was the major contribution to the total removal of HA. In the presence of HA, the holes can produce •OH radicals (reaction (4.2)), which can further degrade the HA into CO_2 and H_2O (reaction (4.3)). Of course, the holes can also directly oxidize the organic molecules (reaction (4.4)). The direct oxidation of HA by positive holes and then the elimination of holes cause a reduction in the electron−hole recombination and thus an increase in the number of electrons that reduce chromium. This results in a photocatalytic efficiency increase in spite of the competition between HA and Cr(VI) for the active sites of TiO_2 (Yang and Lee 2006, D. C. Cid, D. C. Grande et al. 2012, Yang, Lee et al. 2012).

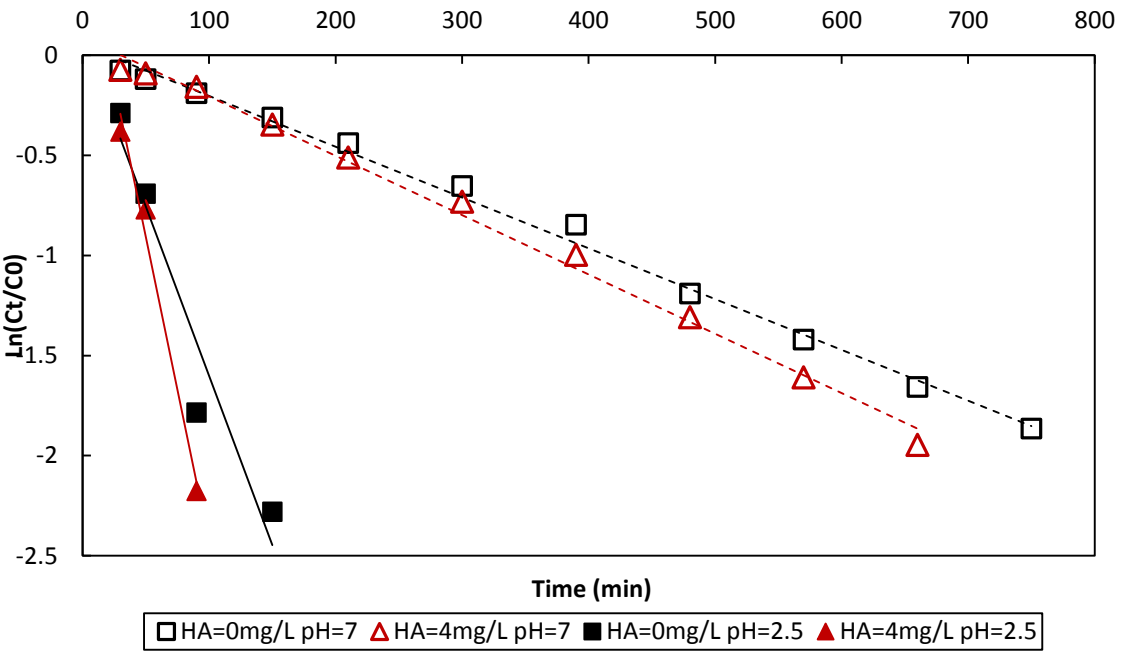

Figure. 4.3.13 The pseudo-first order kinetics plots for Cr(VI) catalytic reduction at pH of 2.5 and 7 under UV+visible light. Effect of HA on the removal of Cr(VI).

Table 4.3.3 kinetic parameters summary

pH	[HA] mg/L	light resorce	K(min^{-1})	R^2
7	0	UV+Visible light	0.0025	0.995
7	4	UV+Visible light	0.0030	0.994
7	0	Visible light	0.0008	0.976
7	4	Visible light	0.0010	0.990
2.5	0	UV+Visible light	0.0169	0.933
2.5	4	UV+Visible light	0.0307	0.984

However, no further enhancement was observed with an increasing concentration of HA. This can be explained by the HA acting as an internal filter (figure 4.3.14), which causes a continuous increase in the absorption of incident UV light with increasing HA concentration (Lin, Wei et al. 1993, Yang and Lee 2006).

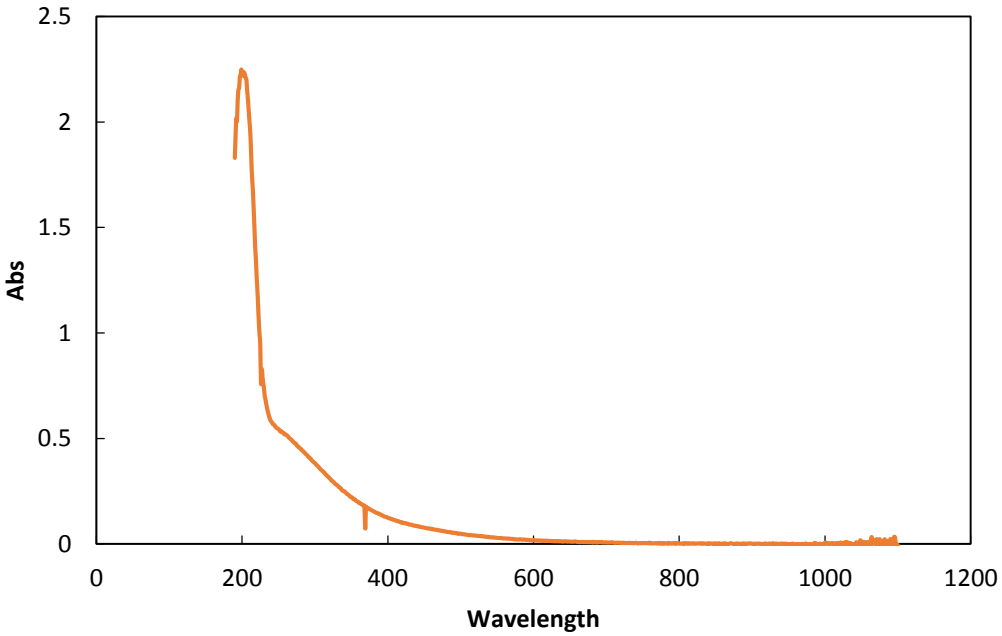

Figure 4.3.14 UV-vis absorbance of humic acid

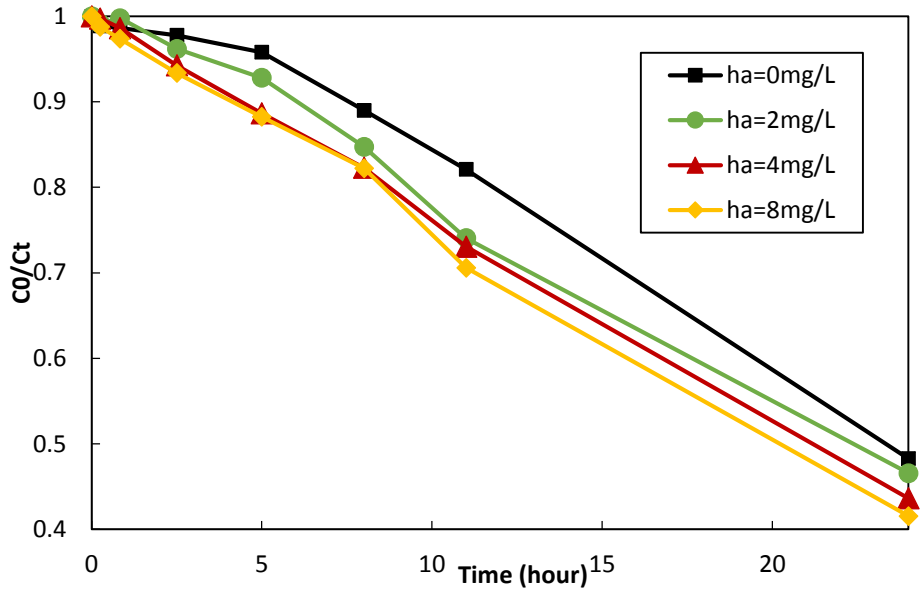

Figure 4.3.15 Effect of HA on Cr(VI) removal under visible light, pH=7.

To understand the role of HA in the Cr(VI) photocatalytic reduction without the interference of strong absorption of UV by HA, we conducted the experiments with HA under visible light illumination. With the visible light, our hypothesis was that the major negative effect of HA on Cr(VI) reduction as previously discussed has been eliminated or minimized. Figure 4.3.15, there is a clear positive correlation between the HA concentration and reaction rates.

The reaction rate increased with an increasing HA concentration under the visible light irradiation, which was different from the results with the UV+ visible light presented earlier. It is likely that because HA absorbs only a very small percentage of visible light as shown in figure 4.3.15, the influence of HA on the visible light density was negligible. However, the improvement for the reaction rate under visible light was still not significant. The specific improved K value is showed in fig 4.3.16 and table 4.3.3. One of the important strategies of promoting the photocatalytic reduction of Cr(VI) is to enhance the charge separation, which can be achieved by improving the structure of the photocatalyst and by

introducing scavengers of holes and/or electrons in the solution via reaction (4.2)-(4.4) (Wang, Wang et al. 2008). The XRD test has already proven the existence of the anatase in the TiO_2/PAN nanofibers. Because of the interaction of anatase phases in nanofibers, it exhibits high activity, which enhances the electron–hole separation and increases the total photoefficiency. A further increase of the electron–hole separation is not expected for TiO_2/PAN nanofibers because it originally provides efficient charge separation (Wang, Wang et al. 2008). Furthermore, the light source has strong influence on the photocatalytic efficiency of the nanofibers. The ability of the HA to reduce the recombination of electron and hole could decline with decreasing photocatalytic efficiency under visible light.

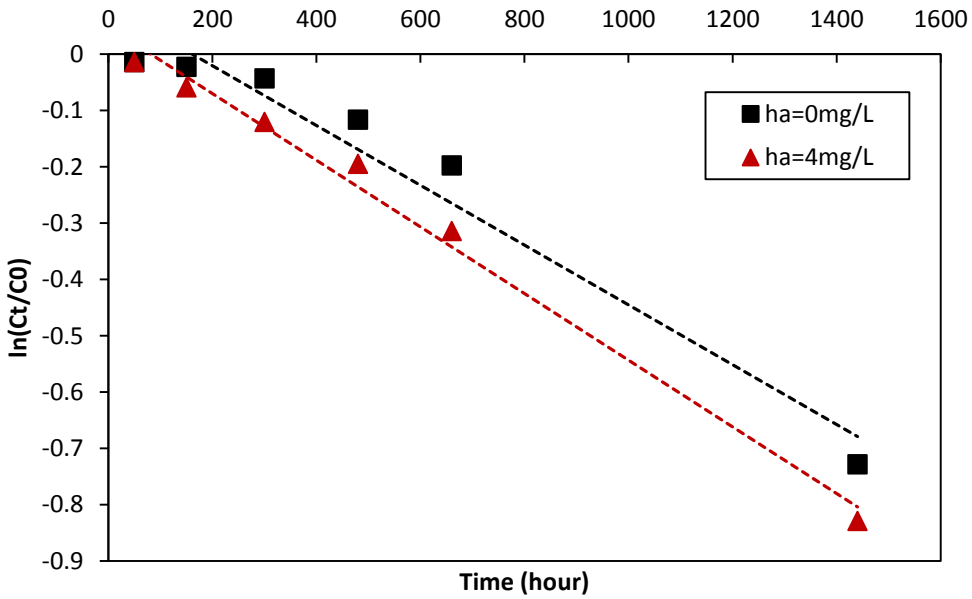

Figure 4.3.16 The pseudo-first order kinetics plots for Cr(VI) catalytic reduction at pH 7 under visible light. Effect of HA on the removal of Cr(VI).

Reference

"Chromium, Hexavalent (Colometric)." U.S. Environmental Protection Agency,Method 218.6; Cincinnati, OH (1992).

"Determination of Cr(VI) in Drinking Water by Ion Chromatography with Post Column Derivatization and UV-visible Spectroscopic Detection." U.S. Environmental Protection Agency,Method 218.6; Cincinnati, OH (2011).

"Determination of Dissolved Hexavalent Chromium in Drinking Water, Groundwater, and Industrial Wastewater Effluents by Ion Chromatography." U.S. Environmental Protection Agency,Method 218.6; Cincinnati, OH (1991).

Anpo, M. (2000). "Utilization of TiO2 photocatalysts in green chemistry." Pure and Applied Chemistry **72**(7): 1265-1270.

Asahi, R., et al. (2001). "Visible-light photocatalysis in nitrogen-doped titanium oxides." Science **293**(5528): 269-271.

Barrera-Diaz, C. E., et al. (2012). "A review of chemical, electrochemical and biological methods for aqueous Cr(VI) reduction." J Hazard Mater **223-224**: 1-12.

Barrera-Díaz, C. E., et al. (2012). "A review of chemical, electrochemical and biological methods for aqueous Cr(VI) reduction." Journal of Hazardous Materials **223-224**: 1-12.

Cappelletti, G., et al. (2008). "Nano-titania assisted photoreduction of Cr(VI). The role of the different TiO2 polymorphs." Applied Catalysis B: Environmental **78**(3-4): 193-201.

Cespón-Romero, R. M., et al. (1996). "Preconcentration and speciation of chromium by the determination of total chromium and chromium(III) in natural waters by flame atomic absorption spectrometry with a chelating ion-exchange flow injection system." Analytica Chimica Acta **327**(1): 37-45.

Chandrasekar, R., et al. (2009). "Fabrication and characterization of electrospun titania nanofibers." Journal of Materials Science **44**(5): 1198-1205.

Chen, X. and S. S. Mao (2007). "Titanium dioxide nanomaterials: Synthesis, properties, modifications and applications." Chemical Reviews **107**(7): 2891-2959.

D. C. Cid, L., et al. (2012). "Removal of Cr(VI) and humic acid by heterogeneous photocatalysis in a laboratory reactor and a pilot reactor." Industrial and Engineering Chemistry Research **51**(28): 9468-9474.

Di Valentin, C., et al. (2007). "N-doped TiO2: Theory and experiment." Chemical Physics **339**(1-3): 44-56.

EPA (2011). "EPA's recommendations for enhanced monitoring for Hexavalent Chromium (Chromium-6) in Drinking Water." **Retrieved**

Giménez, J., et al. (1996). "Photocatalytic reduction of chromium(VI) with titania powders in a flow system. Kinetics and catalyst activity." Journal of Molecular Catalysis A: Chemical **105**(1-2): 67-78.

Greiner, A. and J. H. Wendorff (2007). "Electrospinning: A fascinating method for the preparation of ultrathin fibers." Angewandte Chemie - International Edition **46**(30): 5670-5703.

He, G., et al. (2013). "Electrospun anatase-phase TiO2 nanofibers with different morphological structures and specific surface areas." Journal of Colloid and Interface Science **398**: 103-111.

Huang, Z. M., et al. (2003). "A review on polymer nanofibers by electrospinning and their applications in nanocomposites." Composites Science and Technology **63**(15): 2223-2253.

Im, J. S., et al. (2008). "Preparation of PAN-based electrospun nanofiber webs containing TiO2 for photocatalytic degradation." Materials Letters **62**(21-22): 3652-3655.

Kabra, K., et al. (2004). "Treatment of hazardous organic and inorganic compounds through aqueous-phase photocatalysis: A review." Industrial and Engineering Chemistry Research **43**(24): 7683-7696.

Kajitvichyanukul, P. and P. Amornchat (2005). "Effects of diethylene glycol on TiO2 thin film properties prepared by sol-gel process." Science and Technology of Advanced Materials **6**(3-4 SPEC. ISS.): 344-347.

Khalil, L. B., et al. (1998). "Photocatalytic reduction of environmental pollutant Cr(VI) over some semiconductors under UV/visible light illumination." Applied Catalysis B: Environmental **17**(3): 267-273.

Khalil, L. B., et al. (1998). "Photocatalytic reduction of environmental pollutant Cr(VI) over some semiconductors under UV/visible light illumination." Applied Catalysis B: Environmental **17**(3): 267-273.

Kim, Y. B., et al. (2010). "Fabrication and characterization of TiO2/poly(dimethyl siloxane) composite fibers with thermal and mechanical stability." Journal of Applied Polymer Science **116**(1): 449-454.

Ku, Y. and I.-L. Jung (2001). "Photocatalytic reduction of Cr(VI) in aqueous solutions by UV irradiation with the presence of titanium dioxide." Water Research **35**(1): 135-142.

Ku, Y. and I. L. Jung (2001). "Photocatalytic reduction of Cr(VI) in aqueous solutions by UV irradiation with the presence of titanium dioxide." Water Research **35**(1): 135-142.

Li, D. and Y. Xia (2003). "Fabrication of titania nanofibers by electrospinning." Nano Letters **3**(4): 555-560.

Lin, W.-Y., et al. (1993). "Photocatalytic reduction and immobilization of hexavalent chromium at titanium dioxide in aqueous basic media." Journal of the Electrochemical Society **140**(9): 2477-2482.

Linsebigler, A. L., et al. (1995). "Photocatalysis on TiO2 surfaces: Principles, mechanisms, and selected results." Chemical Reviews **95**(3): 735-758.

Mu, R., et al. (2010). "On the photocatalytic properties of elongated TiO2 nanoparticles for phenol degradation and Cr(VI) reduction." Journal of Hazardous Materials **176**(1-3): 495-502.

Nguyen, H. Q. and B. Deng (2012). "Electrospinning and in situ nitrogen doping of TiO2/PAN nanofibers with photocatalytic activation in visible lights." Materials Letters **82**(0): 102-104.

Pifferi, V., et al. (2013). "Electrodeposited nano-titania films for photocatalytic Cr(VI) reduction." Catalysis Today **209**: 8-12.

Prairie, M. R., et al. (1993). "An investigation of TiO2 photocatalysis for the treatment of water contaminated with metals and organic chemicals." Environmental Science and Technology **27**(9): 1776-1782.

Prairie, M. R., et al. (1993). "An investigation of TiO2 photocatalysis for the treatment of water contaminated with metals and organic chemicals." Environmental Science and Technology **27**(9): 1776-1782.

Shaham Waldmann, N. and Y. Paz (2010). "Photocatalytic reduction of cr(VI) by titanium dioxide coupled to functionalized cnts: An example of counterproductive charge separation." Journal of Physical Chemistry C **114**(44): 18946-18952.

Wan Ngah, W. S. and M. A. K. M. Hanafiah (2008). "Removal of heavy metal ions from wastewater by chemically modified plant wastes as adsorbents: A review." Bioresource Technology **99**(10): 3935-3948.

Wang, L., et al. (2008). "Photocatalytic reduction of Cr(VI) over different TiO2 photocatalysts and the effects of dissolved organic species." Journal of Hazardous Materials **152**(1): 93-99.

Yang, J. K. and S. M. Lee (2006). "Removal of Cr(VI) and humic acid by using TiO2 photocatalysis." Chemosphere **63**(10): 1677-1684.

Yang, J. K., et al. (2012). "Effect of different types of organic compounds on the photocatalytic reduction of Cr(VI)." Environmental Technology (United Kingdom) **33**(17): 2027-2032.

Yoneyama, H., et al. (1979). "Heterogeneous photocatalytic reduction of dichromate on n-type semiconductor catalysts [5]." Nature **282**(5741): 817-818.

Yu, H., et al. (2007). "Photocatalytic activity of the calcined H-titanate nanowires for photocatalytic oxidation of acetone in air." Chemosphere **66**(11): 2050-2057.

Zhang, C., et al. (2012). "Polyacrylonitrile/manganese acetate composite nanofibers and their catalysis performance on chromium (VI) reduction by oxalic acid." J Hazard Mater **229-230**: 439-445.

Ziabicki, A. (1976). Fundamentals of fibre formation: the science of fibre spinning and drawing.

Chapter 5 CONCLUSIONS AND PERSPECTIVE

5.1 Conclusions

Visible light activated TiO_2/PAN nanofibers was successfully prepared by the electrospinning process. The application of TiO_2/PAN nanofibers on the photocatalytic reduction of Cr(VI) in the aqueous solution at different conditions has been examined. The photocatalytic reaction of Cr(VI) is highly pH sensitive. The reaction rate of Cr(VI) increases with decreasing pH, likely because of the higher thermodynamic driving force for the reduction of Cr(VI) at lower pH. The as-prepared nanofibers had an excellent ability to catalyze Cr(VI) reduction at acid conditions. At acidic and neutral condition, the removal efficiency was nearly 100% under both UV and visible light exposure, which partially confirm that TiO_2 anatase crystals had been doped to some degree with carbon or nitrogen in the annealing process. The reaction rate of Cr(VI) was enhanced when the system containing both HA and Cr(VI) when compared to the system with Cr(VI) alone. This trend could be resulted from the increased photocatalytic efficiency due to the reduced recombination between positive holes in the valence band and the electrons in the conduction band of the TiO_2. Moreover, the TiO_2/PAN nanofibers mat had good stability and durability in the application. The used nanofibers recovered from the solution with pH of 2.5 preformed as well as the original TiO_2/PAN nanofibers. Overall, this research suggests that the photocatalytic reaction using illuminated TiO_2/PAN nanofibers could be applied to the treatment of wastewaters containing both Cr(VI) and possible organic compounds.

5.2 Recommendation and future research

Photocatalytic oxidation of the organic contaminants (e.g. benzene, toluene, ethyl benzene, and m-xylene) via TiO_2/PAN nanofibers was investigated by Nguyen and Deng (Nguyen and Deng 2012). Cr(VI) phototcatalytic reduction with this material has been studied in this research as well. The applications of TiO_2/PAN nanofibers for the treatment of other inorganic compounds such as Cu(II), Hg(II), Pb(II) is appropriate for the further investigation.

Further improvement of physical properties and photocatalytic efficiency of modified TiO_2 nanofibers is desirable. As referred to the previous chapter, in order to get the higher mechanical strength, the nanofibers could become less porous. Therefore, the specific surface area of the TiO_2/PAN nanofibers was much lower than the other TiO_2 nanomaterial, which led to the negative effect on its photocatalytic efficiency. The future study could focus on improving the synthesis process for the TiO_2 nanofibers so as to enlarge the specific surface area of the nanofibers and to keep or enhance the physical properties of the nanofibers at the same time. In the literature review part of chapter 2, I mentioned that the metal dopants exhibits better ability for the activation of TiO_2 with visible light. It is therefore expected that the addition of these materials as the alternative dopants for the TiO_2 nanofibers through proper method will be a valuable and promising research objective. Furthermore, the recovery of the catalyst is one of the vital factors for its potential application, and current study indicates that the Cr(III) could be easily precipitated on the surface of TiO_2 at higher pH value. A flow-through system could potentially eliminate or decrease fouling of the solid TiO_2-photocataytic materials, so should be investigated further.

Appendix

- Adsorption of Cr(VI) on TiO_2/PAN Nanofibers

		pH=2.5		pH=5.0		pH=7.0		pH=8.5	
Time(hr)	(min)	A	Ct/c0	A	Ct/c0	A	Ct/c0	A	Ct/c0
0	0	0.806	1.000	0.807	1.000	0.796	1.000	0.793	1.000
0.5	30	0.799	0.991	0.803	0.995	0.799	1.004	0.793	1.000
1.5	90	0.800	0.993	0.788	0.976	0.776	0.975	0.789	0.995
2.5	150	0.796	0.988	0.783	0.970	0.795	0.999	0.792	0.999
5	300	0.791	0.981	0.781	0.968	0.798	1.003	0.783	0.987
8	480	0.792	0.983	0.779	0.965	0.787	0.989	0.781	0.985
14	840	0.794	0.985	0.790	0.979	0.785	0.986	0.785	0.990
24	1440	0.786	0.975	0.778	0.964	0.781	0.981	0.792	0.999
48	2880	0.782	0.970	0.773	0.958	0.772	0.970	0.768	0.968
72	4320							0.764	0.963

- Variation of reaction system temperature

Time(min)	T(c)	T(K)
0	22.5	295.5
5	32	305
10	37	310
20	40.5	313.5
30	42	315
45	42	315

- Influence of pH (UV+visible light, virgin nanofibers)

	pH=2.5		pH=5.0	
Time(min)	Ct/c0	ln(Ct/C0)	Ct/c0	ln(Ct/C0)
0	1.000	0.000	1.000	0.000
5	0.923	-0.080	0.963	-0.037
15	0.852	-0.160	0.895	-0.111
30	0.749	-0.289	0.843	-0.171
50	0.501	-0.691	0.714	-0.338
90	0.168	-1.784	0.544	-0.610
150	0.102	-2.281	0.391	-0.939
210	0.003	-5.881	0.201	-1.604
270			0.110	-2.204
330			0.006	-5.049
390			0.006	-5.116

pH=7.0			pH=8.5		
Time(min)	Ct/c0	ln(Ct/C0)	Time(min)	Ct/c0	ln(Ct/C0)
0	1.000	0.000	0	1.000	0.000
5	0.986	-0.014	5	0.975	-0.026
15	0.966	-0.034	15	0.967	-0.033
30	0.927	-0.076	30	0.955	-0.046
50	0.887	-0.119	50	0.951	-0.051
90	0.827	-0.190	90	0.931	-0.071
150	0.733	-0.311	150	0.896	-0.109
210	0.645	-0.439	210	0.839	-0.176
300	0.520	-0.654	300	0.786	-0.241
390	0.429	-0.847	390	0.666	-0.406
480	0.304	-1.190	480	0.584	-0.537
570	0.241	-1.421	660	0.545	-0.608
660	0.191	-1.656	840	0.436	-0.830
750	0.155	-1.866	1020	0.381	-0.966
840	0.113	-2.177	1200	0.307	-1.180
930	0.065	-2.728	1560	0.253	-1.374
1020	0.058	-2.728	1920	0.210	-1.562
1440	0.051	-2.970	2280	0.204	-1.592
2880	0.051	-2.980	2880	0.199	-1.615
4320	0.050	-2.990	4320	0.199	-1.615

- Influence of pH (UV+visible light, recovered nanofibers)

	pH=2.5		pH=5.0	
Time(min)	A	Ct/c0	A	Ct/c0
0	0.652	1.000	0.820	1.000
5	0.625	0.959	0.825	1.006
15	0.571	0.876	0.803	0.979
30	0.480	0.736	0.769	0.938
50	0.305	0.468	0.678	0.827
90	0.173	0.265	0.616	0.751
150	0.081	0.124	0.562	0.685
210	0.043	0.066	0.426	0.520
270			0.282	0.344
330			0.167	0.204

- Visible light

pH=2.5			pH=5		
Time(min)	Ct/c0	ln(Ct/C0)	Time(min)	Ct/c0	ln(Ct/C0)
0	1.000	0.000	0	1.000	0.000
5	0.957	-0.044	5	0.994	-0.006
15	0.939	-0.063	15	0.930	-0.072
30	0.901	-0.104	30	0.902	-0.104
50	0.838	-0.177	50	0.882	-0.125
90	0.700	-0.357	90	0.813	-0.207
150	0.482	-0.730	150	0.711	-0.342
210	0.240	-1.428	210	0.610	-0.495
270	0.023	-3.870	300	0.486	-0.721
330	0.004	-5.546	390	0.401	-0.914
			480	0.232	-1.462
			570	0.095	-2.356
			660	0.008	-4.779

pH=7.0			pH=8.5		
Time(min)	ct/c0	ln(Ct/C0)	Time(min)	ct/c0	ln(Ct/C0)
0	1.000	0.000	0	1.000	0.000
15	0.989	-0.011	150	0.922	-0.081
50	0.986	-0.014	300	0.903	-0.102
90	0.981	-0.019	480	0.883	-0.124
150	0.978	-0.022	660	0.857	-0.154
300	0.958	-0.043	1440	0.791	-0.235
480	0.890	-0.116	2880	0.605	-0.503
660	0.821	-0.197	4320	0.555	-0.590
1020	0.642	-0.443	5760	0.558	-0.584
1440	0.483	-0.728			
1800	0.325	-1.125			
2160	0.214	-1.544			
2520	0.162	-1.822			
2880	0.120	-2.122			
3240	0.094	-2.366			
3600	0.070	-2.654			
3960	0.053	-2.936			
4320	0.048	-3.033			

- The impact of humic acid (HA)

Without nanofibers (UV+visible light irradiation)

HA(TOC)=2mg/L		pH=7
Time(min)	A	Ct/C0
0	0.83	1.000
50	0.825	0.994
150	0.813	0.980
300	0.81	0.976
480	0.806	0.971
660	0.808	0.973
840	0.799	0.963
1440	0.794	0.957

Adsorption (with nanofibers, in dark)

HA(TOC)=2mg/L		pH=7
Time(min)	A	Ct/C0
0	0.764	1.000
50	0.766	1.003
150	0.757	0.991
300	0.759	0.993
480	0.751	0.983
660	0.756	0.990
840	0.753	0.986
1440	0.748	0.979

Various HA TOC (UV+visible light, pH=7)

pH=7	HA=2 mg/L		HA= 4 mg/L		HA=8 mg/L	
Time(min)	Ct/C0	ln(Ct/C0)	Ct/C0	ln(Ct/C0)	Ct/C0	ln(Ct/C0)
0	1.000	0.000	1.000	0.000	1.000	0.000
5	0.976	-0.025	0.965	-0.036	0.987	-0.013
15	0.956	-0.045	0.949	-0.052	0.971	-0.030
30	0.930	-0.073	0.929	-0.073	0.951	-0.050
50	0.891	-0.115	0.914	-0.090	0.920	-0.084
90	0.826	-0.191	0.855	-0.157	0.862	-0.149
150	0.772	-0.259	0.707	-0.346	0.741	-0.300
210	0.682	-0.383	0.600	-0.511	0.628	-0.465
300	0.493	-0.707	0.481	-0.731	0.475	-0.744
390	0.396	-0.926	0.369	-0.997	0.296	-1.216
480	0.233	-1.455	0.270	-1.309	0.256	-1.363
570	0.185	-1.688	0.200	-1.609	0.205	-1.585
660	0.129	-2.051	0.143	-1.947	0.191	-1.655
750	0.084	-2.476	0.105	-2.250	0.148	-1.909
840	0.072	-2.630	0.073	-2.624	0.095	-2.351

Various HA TOC (UV+visible light, pH=2.5)

pH=2.5	HA=2 mg/l		HA=4 mg/l		HA=8 mg/l	
Time(min)	Ct/C0	ln(Ct/C0)	Ct/C0	ln(Ct/C0)	Ct/C0	ln(Ct/C0)
0	1.000	0.000	1.000	0.000	1.000	0.000
5	0.940	-0.062	0.943	-0.058	0.921	-0.083
15	0.867	-0.143	0.830	-0.187	0.790	-0.235
30	0.687	-0.376	0.671	-0.399	0.578	-0.548
50	0.436	-0.829	0.387	-0.949	0.360	-1.021
90	0.101	-2.293	0.113	-2.176	0.090	-2.403
150	0.012	-4.396	0.004	-5.577	0.003	-5.900

Various HA TOC (Visible light, pH=7)

pH=7	HA=2 mg/L		HA= 4 mg/L		HA=8 mg/L	
Time(hr)	Ct/C0	ln(Ct/C0)	Ct/C0	ln(Ct/C0)	Ct/C0	ln(Ct/C0)
0.00	1.000	0.000	1.000	0.000	1.000	0.000
0.25	0.991	-0.009	0.998	-0.002	0.987	-0.013
0.83	0.998	-0.002	0.986	-0.014	0.974	-0.027
2.50	0.962	-0.039	0.943	-0.059	0.934	-0.069
5.00	0.928	-0.075	0.887	-0.120	0.882	-0.125
8.00	0.847	-0.166	0.823	-0.195	0.822	-0.196
11.00	0.740	-0.300	0.731	-0.314	0.706	-0.348
24.00	0.466	-0.764	0.436	-0.829	0.416	-0.878